

U.S.N.A. --- Trident Scholar Report; no. 341 (2005)

**Analysis, Fabrication, and Testing of a Composite Bladed Propeller
For a Naval Academy Yard Patrol (YP) Craft**

By

Midshipman 1/c Christopher D. Wozniak, Class of 2005
United States Naval Academy
Annapolis, MD

(Date)

Certification of Adviser Approval

Associate Professor Paul H. Miller
Naval Architecture & Ocean Engineering Department

(Date)

Acceptance for the Trident Scholar Committee

Professor Joyce E. Shade
Deputy Director of Research

(Date)

REPORT DOCUMENTATION PAGE

Form Approved
OMB No. 074-0188

Public reporting burden for this collection of information is estimated to average 1 hour per response, including the time for reviewing instructions, searching existing data sources, gathering and maintaining the data needed, and completing and reviewing the collection of information. Send comments regarding this burden estimate or any other aspect of the collection of information, including suggestions for reducing this burden to Washington Headquarters Services, Directorate for Information Operations and Reports, 1215 Jefferson Davis Highway, Suite 1204, Arlington, VA 22202-4302, and to the Office of Management and Budget, Paperwork Reduction Project (0704-0188), Washington, DC 20503.

1. AGENCY USE ONLY (Leave blank)		2. REPORT DATE 6 May 2005	3. REPORT TYPE AND DATE COVERED	
4. TITLE AND SUBTITLE Analysis, fabrication, and testing of a composite bladed propeller for a Naval Academy Yard Patrol (YP) craft			5. FUNDING NUMBERS	
6. AUTHOR(S) Wozniak, Christopher D. (Christopher David), 1982-				
7. PERFORMING ORGANIZATION NAME(S) AND ADDRESS(ES)			8. PERFORMING ORGANIZATION REPORT NUMBER	
9. SPONSORING/MONITORING AGENCY NAME(S) AND ADDRESS(ES) US Naval Academy Annapolis, MD 21402			10. SPONSORING/MONITORING AGENCY REPORT NUMBER Trident Scholar project report no. 341 (2005)	
11. SUPPLEMENTARY NOTES				
12a. DISTRIBUTION/AVAILABILITY STATEMENT This document has been approved for public release; its distribution is UNLIMITED.			12b. DISTRIBUTION CODE	
13. ABSTRACT: The U.S. Navy, and much of the maritime industry, uses nickel-aluminum-bronze (NAB) as the primary material for propeller construction. This is done for many reasons, including its anti-biofouling characteristics, high stiffness, and low corrosion potential. However, NAB is a cathodic metal. While it experiences little corrosion itself, its presence leads to galvanic corrosion of the surrounding hull steel. The U.S. Navy, and much of the maritime industry, uses nickel-aluminum-bronze (NAB) as the primary material for propeller construction. This is done for many reasons, including its anti-biofouling characteristics, high stiffness, and low corrosion potential. However, NAB is a cathodic metal. While it experiences little corrosion itself, its presence leads to galvanic corrosion of the surrounding hull steel. The Navy has considered the feasibility of a composite bladed propeller design, but several variables need investigation. The goal of this Trident project was to design, build and test the Navy's first composite propeller. The detailed objectives of the research were to: evaluate a hub design; perform a structural design of a Yard Patrol (YP) craft composite bladed propeller; and finally, build and test a full-scale propeller using the composite materials. As the general concept used composite blades attached to a NAB hub, the first step was to develop a design for the hub-blade interaction. Afterwards, the loads were predicted using computational fluid dynamics. The pressure plot was then combined with the geometry in a finite element structural analysis program to determine fiber orientation and strength characteristics. A full-scale mold plug was created using stereolithography. Finally, the carbon/epoxy blades were laid up in this mold. The YP craft was selected as the test platform as it: 1) has two propellers (in the event of failure); and 2) is used for many hours, often in harsh conditions. Testing included: 1) benchmarking the standard NAB propellers; 2) installing and evaluating new polyurea-encapsulated propellers developed by the Naval Surface Warfare Center-Carderock; and, 3) evaluation of the composite bladed propeller. This project holds definite promise for the future of propulsor technology, with specific application to submarine vehicles. The potential for this technology to reduce cavitation, noise, mass and cost, could significantly improve U.S. naval vessels.				
14. SUBJECT TERMS: Composite, Yard Patrol, propeller, stereolithography			15. NUMBER OF PAGES 118	
			16. PRICE CODE	
17. SECURITY CLASSIFICATION OF REPORT		18. SECURITY CLASSIFICATION OF THIS PAGE	19. SECURITY CLASSIFICATION OF ABSTRACT	20. LIMITATION OF ABSTRACT

Abstract

The U.S. Navy, and much of the maritime industry, uses nickel-aluminum-bronze (NAB) as the primary material for propeller construction. This is done for many reasons, including its anti-biofouling characteristics, high stiffness, and low corrosion potential. However, NAB is a cathodic metal. While it experiences little corrosion itself, its presence leads to galvanic corrosion of the surrounding hull steel.

The Navy has considered the feasibility of a composite bladed propeller design, but several variables need investigation. The goal of this Trident project was to design, build and test the Navy's first composite propeller. The detailed objectives of the research were to: evaluate a hub design; perform a structural design of a Yard Patrol (YP) craft composite bladed propeller; and finally, build and test a full-scale propeller using the composite materials.

As the general concept used composite blades attached to a NAB hub, the first step was to develop a design for the hub-blade interaction. Afterwards, the loads were predicted using computational fluid dynamics. The pressure plot was then combined with the geometry in a finite element structural analysis program to determine fiber orientation and strength characteristics. A full-scale mold plug was created using stereolithography. Finally, the carbon/epoxy blades were laid up in this mold.

The YP craft was selected as the test platform as it: 1) has two propellers (in the event of failure); and 2) is used for many hours, often in harsh conditions.

Testing included: 1) benchmarking the standard NAB propellers; 2) installing and evaluating new polyurea-encapsulated propellers developed by the Naval Surface Warfare Center-Carderock; and, 3) evaluation of the composite bladed propeller.

This project holds definite promise for the future of propulsor technology, with specific application to submarine vehicles. The potential for this technology to reduce cavitation, noise, mass and cost, could significantly improve U.S. naval vessels.

Keywords: Composite, Yard Patrol, propeller, stereolithography

Table of Contents

INTRODUCTION	8
BACKGROUND AND THEORY	10
Hub and Blades	10
Finite Element Analysis (FEA)	13
Propeller Theory and Design Philosophy	14
Concepts and Materials	17
Encapsulation	18
Encapsulation	19
Composite Materials	22
Propeller Blade and Hub Fabrication	31
METHODS OF EXPERIMENTATION	34
Coupon Testing	34
Full-Scale Testing	35
Fiber Optic Strain Gaging	36
DOVETAIL DESIGN AND LOAD GENERATION	41
Dovetail Design	41
Load Generation	45
FINITE ELEMENT ANALYSIS	49
NAB Propellers	49
Encapsulated Propellers	54
Composite Bladed Propeller	57
NAB Hub	63
FABRICATION	65
NAB Hub	65

Composite Blades	4 67
FULL SCALE TESTING	73
Bronze and Encapsulated Propellers	73
Composite Bladed Propeller	83
CONCLUSIONS AND RESULTS	85
NOTES	88
WORKS CITED	90
APPENDIX A – TEST COUPON PROTOCOL	92
APPENDIX B – DOVETAIL GENERATION PROGRAM	95
APPENDIX C – FACTOR OF SAFETY INFORMATION	97
APPENDIX D – YP TEST PLAN	98
APPENDIX E – DATA ANALYSIS CODE	108

Table of Figures

FIGURE 1 – Joint Concepts	10
FIGURE 2 – Dovetail Detail	10
FIGURE 3 – Tip Cavitation	16
FIGURE 4 – Encapsulated Propeller	19
FIGURE 5 – Starboard Encapsulated Propeller	20
FIGURE 6 – YP Propeller Mold	20
FIGURE 7 – Dovetail Hub Acrylic Model	32
FIGURE 8 – Test Coupon Displacement Plot	39
FIGURE 9 – Hub and Blade Model	43
FIGURE 10 – Blade/Hub Rendering	44
FIGURE 11 – Bronze Stress Plot	52
FIGURE 12 – Encapsulated Propellers on YP677	54
FIGURE 13 – Through the Thickness Stress Plot	61
FIGURE 14 – Stress Riser at Keyway/Dovetail	63
FIGURE 15 – NAB Hub	65
FIGURE 16 – NAB Hub	65
FIGURE 17 – Plug and Flange	67
FIGURE 18 – Mold Fabrication Setup	68
FIGURE 19 – Cutting Area	69
FIGURE 20 – Ply Stacks	69
FIGURE 21 – Laminating	70

FIGURE 22 – Open Water Efficiency vs. Percent Increase of Thickness to Diameter Ratio	71
FIGURE 23 – Shaft Access	73
FIGURE 24 – Flex Coupling	74
FIGURE 25 – Brake Horsepower vs. Engine RPM for Baseline Test	77
FIGURE 26 – Brake Horsepower vs. Engine RPM for Encapsulated Test	78
FIGURE 27 – RPM Calibration Results (Encapsulated Propellers)	80
FIGURE 28 – Composite Propeller Installation	83
FIGURE 29 – Composite Propeller Test Results	83
FIGURE 30 – Installed Composite Bladed Propeller	84
FIGURE 31 – Wake of Yard Patrol Craft at Flank Speed	84

Note: All stress units are in pounds per square inch (psi),
all length units are in inches (in), and all load units are in pounds (lbs).

Acknowledgments

I would like to thank: Dr. Paul Miller for all of his help and support in this project, as well as his wife Dawn, Dr. Joyce Shade, Dr. Sarah Mouring and the Trident Committee, Dr. Richard Szwerc and all of the members of his code at NSWCCD, Mr. Edward Gerding and his team from Boeing, Mr. Tom Price and the personnel in the TSD shop, Mr. John Hill and the personnel in the Hydromechanics Lab, Mr. Tom Carr, ENCS Timothy Grau, and BMC Kenneth Mills from NAVSTA Annapolis, as well as MIDN 1/c Michael Sammataro, MIDN 1/c John Coombs, Midn 1/c Philip Suchyta, and MIDN 1/c Seth Krueger. Without the support and encouragement of these individuals, this research would have remained a distant dream . . .

Introduction

For thousands of years, the ocean and the wonders it holds has intrigued mankind. Across these wide expanses of water existed foreign lands; land which was thought to possess many valuable trade items. However, there were no bridges and the monetary and time investment was too great to successfully use land routes. How could man quench his need for maritime travel? Water-borne vehicles had potential, but powering them was a hurdle. There was a progression from oars and paddles, to sails, to paddlewheels and eventually the screw propeller – the primitive ancestor of what most ships to this day.

While man's curiosity grew with regard to different propulsion methods, so did the experimentation with materials: wood and later aluminum, steel, and then fiberglass and carbon fiber. While the technology behind the propulsor – both in design and powering – has developed with great leaps, the materials used in modern screw propellers have strayed little from what has become the standard: nickel-aluminum-bronze (NAB).

Foreign navies have begun to experiment with composite materials in propeller structures, yet the U.S. has not gone far beyond the NAB frontier. The potential exists, both in technology and resources, for the U.S. Navy to realize the benefits of this concept. Perhaps the U.S. Naval Academy's Yard Patrol craft should be the vessel to bring naval propulsion into the 21st century.

A composite bladed design has several inherent benefits due to its material properties. AIR Fertigung – Technologie GmbH in Rostock, Germany reports in *Ship and Boat International* that the propellers they have put into service have increased strength, fuel efficiency, and acceleration while virtually eliminating cavitation and galvanic corrosion of the

hull (due to the inert quality of the epoxy).¹ Dr. Richard Szwerc and his team at Naval Surface Warfare Center - Carderock Division (NSWCCD) are particularly interested in proving that a composite bladed design can work as well as an NAB model on a naval vessel. His experimentation was postponed, to some extent due to the events of the 11 September 2001. The objective of this Trident project was to take the resources available and provide feedback to NAVSEA on how the composite bladed design performed and whether it truly had the potential reported by the AIR corporation and its competition. Intermediate goals included: learning the basics of propeller design, computer aided design, computational fluid dynamics, and finite element analysis; project management skills; gaining knowledge of composite materials, their related fabrication processes, and composite component design; and, the formulation and execution of an inclusive test regimen from which accurate results could be provided to NAVSEA as a by-product of the in-house educational and research experience.

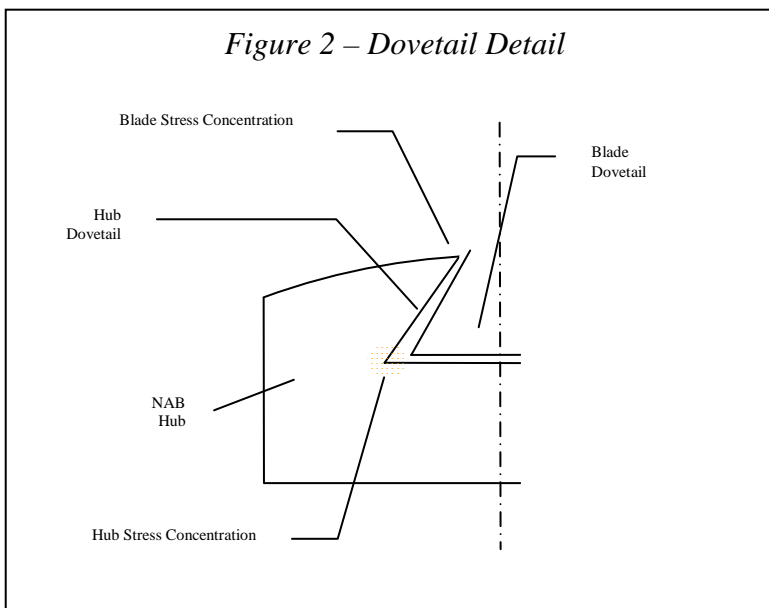
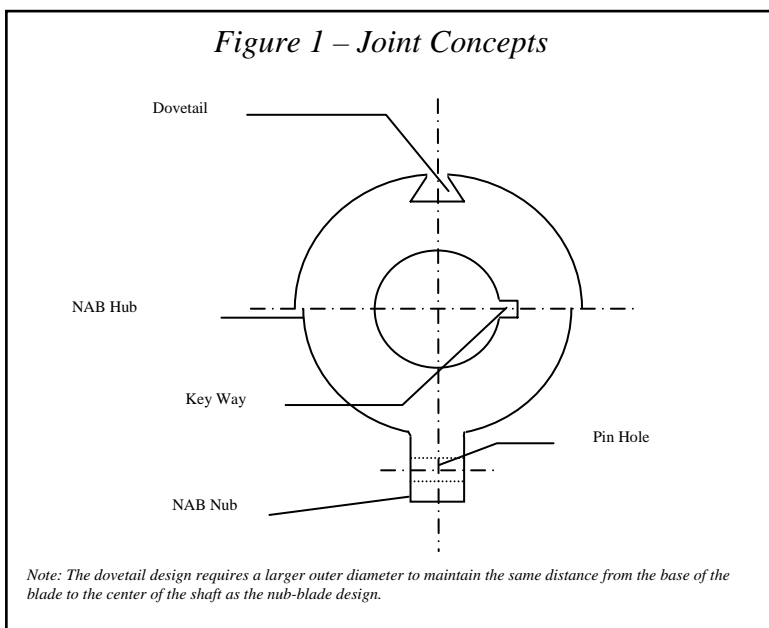
Perhaps composite bladed propeller technology could be the next leap in making our submarines more stealthy, extending the service life of our surface vessel propulsion systems, and increasing speed and range of our fast attack/littoral combat ships. The research accomplished in this project will hopefully be an integral part of the foundation needed to make composite propeller technology in the U.S. Navy a reality.

Background and Theory

Hub and Blades

The logical place to begin this feasibility study was the hub section of the propeller, as all of the blades connect in this region. There were two main conceptual designs that were nominally considered within the scope of this Trident project: one was the interlocking “dovetail” (female) design and the other was a “nub-blade” (male) design.

The interlocking dovetail hub (Figure 1) is a design used by the AIR corporation. This particular method allows the



vessel’s operators to easily replace blades in the event of damage or end of life cycle maintenance by simply sliding the blade from the hub. This method of replacement and maintenance is certainly easier than with a solid piece NAB propeller. If a single-piece propeller is damaged, the entire propeller must be taken off, then repaired or replaced. With a composite

bladed design, repair is done on a per blade basis. A benefit of this design is its reliance on a purely physical attachment, instead of using mechanical fasteners such as rivets or a bolt mechanism, similar to what is necessary in the nub-blade design. Sliding the blade into the hub would eliminate the stress concentration produced by a through-blade attachment apparatus; however, a new stress concentration region develops where the blade makes contact with the hub along the hub's outer perimeter. Figure 2 shows the stress concentration regions for the hub as well as the propeller blades.

The nub-blade design works by sliding the composite blade onto what could be considered a much smaller NAB blade (Figure 1). One or two pins connect the blade and hub, posing another problem. Holes must be drilled through the composite material for the connection pins, thus forming significant stress concentrations in the blade as well as the hub. Such a design change would shift the focus from failure by fatigue or impact to failure by overloading. The stress concentration factor is a function of the "sharpness" of the cut made and its length, given by Equation (1).²

$$SCF = 2\sqrt{\frac{a}{\rho_t}} \quad (1)$$

Where:

SCF = Stress Concentration Factor

ρ_t = crack tip radius

a = half of the crack length

This is the general equation for the stress concentration factor, but if the "crack" is circular, ρ_t and a are the same; thus, the SCF would equal two. Furthermore, depending on the

size of the hole, the stress experienced at that blade cross-section could be more than double what a non-pierced section would encounter (as evidenced by Equation (2)).³

$$\sigma = SCF \frac{My}{I} \quad (2)$$

Where:

σ = stress due to bending

SCF = Stress Concentration Factor

M = maximum bending moment

y = distance from the neutral axis to farthest fiber

I = Moment of Inertia of element cross-section

The cross-sectional moment of inertia also decreases due to the bored hole. The end result is a combined stress at the drilled cross-section that is over twice what would have occurred in an entirely intact blade. Such a factor is worth consideration.

Finite Element Analysis (FEA)

Propeller blades experience a wide variety of stresses and deflections due to the various flow conditions while moving a vessel through the water. Analysis becomes more difficult due to the complex nature of how the corresponding loads are applied in the three-dimensional realm. To design for these load cases, the finite element analysis (FEA) method was used to determine modes of failure and overcome certain weaknesses in the design before fabrication. FEA, as described by Niels Ottosen and Hans Petersson, is essentially a computer program designed to approximate the differential equations related to these complex stress states over small areas of the material, or finite elements.⁴ Assembling these elements allows the user to view a representation of a proscribed event or load case. In order for the program to work correctly, however, the user must input certain conditions such as material properties, geometry, assumed loads, and boundary conditions (means of restricting the object's movements).

In the case of the YP propeller, FEA was vital to the material engineering and design. Using a composite material such as carbon cloth does not correlate directly to nickel-aluminum-bronze or steel. Material differences such as stiffness and hardness come into play in a structure that is similar, in some respects, to a cantilever beam under a distributed load. The stiffness affects the deflection of the blade over its length, a characteristic of special interest in propeller design. What FEA offers is a look at how the blades will act, comparatively, under load. Additionally, it allows the materials to be oriented in such a manner as to prevent overload failure. There are often more unknowns in composite engineering than in structural designs using aluminum or steel alloys. Finite element analysis explores some of these unknowns at the user's demand, before the actual fabrication takes place – saving both time and money as the design progresses.

Propeller Theory and Design Philosophy

A vessel's propeller is essentially a set of lifting surfaces, similar to airfoils or wings, mounted in a radial fashion on a hub. As it rotates through the water, a pressure differential is produced such that an area of low pressure forms on the forward face of the blade (suction side) and a high pressure region is developed on the back (pressure side). This situation creates a force pushing the propeller, and therefore the vessel, in the forward direction. The resultant force is defined as thrust.

Just as in ship design and construction, it is too costly to routinely produce full-scale prototype propellers and test them on their design platforms. Instead, open-water scale testing in a towing tank is used to produce non-dimensional propeller coefficients for thrust and torque, represented by the variables K_T and K_Q . Equations (3) and (4) indicate that these coefficients are found using the thrust or torque produced (respectively) as well as the size of the propeller, the fluid density, and the rotational speed.⁵

$$K_T = \frac{T}{\rho n^2 D^4} \quad (3)$$

$$K_Q = \frac{Q}{\rho n^2 D^5} \quad (4)$$

Where:

K_T = thrust coefficient

T = thrust

ρ = density of fluid

n = rotational velocity

K_Q = torque coefficient

Q = torque

D = propeller diameter

Initially, the plan for this Trident project was to gather open-water data from a scale propeller, as well as a circulating water channel cavitation study. However, due to the operational status of the 380-foot Naval Academy Hydromechanics Laboratory (NAHL) towing tank, the open-water experimentation was not completed. The discussion of these principles remains important. If the towing tank was in working order, a full set of NAB versus composite bladed open-water tests were scheduled to determine their hydrodynamic similarities. A curve plotting the K_Q , K_T , and η_0 values as a function of J would have been generated from these tests, where J is defined as the advance ratio (Equation (5)) and η_0 is the open-water efficiency of the propeller (Equation (6)).⁶ However, the open-water efficiency is not synonymous with the ship's overall propulsive efficiency, as it is derived from open-water, uninterrupted fluid trials – flow conditions more ideal than those experienced by a ship-mounted propeller. The open-water efficiency allows the two propellers to be compared in a controlled flow environment.

$$J = \frac{V_A}{nD} \quad (5)$$

$$\eta_0 = \frac{J}{2\pi} \times \frac{K_T}{K_Q} \quad (6)$$

Where:

J = advance ratio

V_A = speed of advance

n = rotational velocity

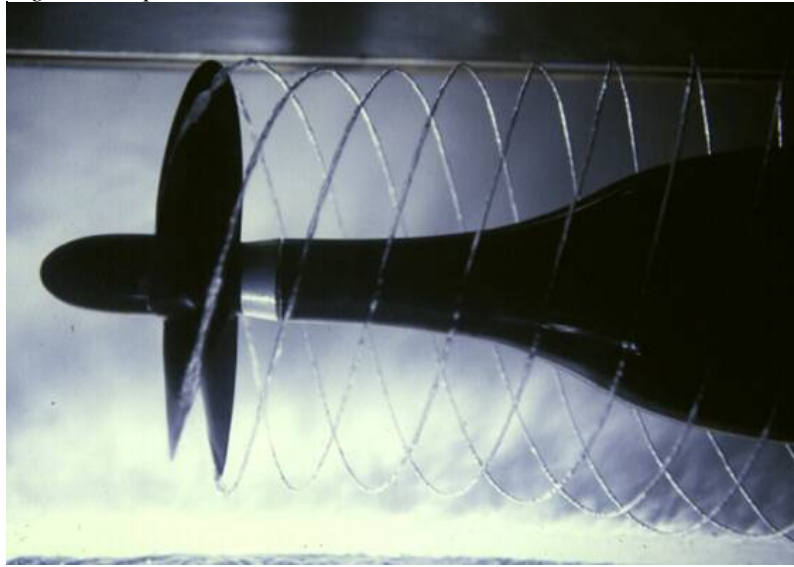
D = propeller diameter

η_0 = open-water efficiency

K_T = thrust coefficient

K_Q = torque coefficient

Figure 3 - Tip Cavitation



A short cavitation study conducted in the Hydromechanics Laboratory circulating water channel was to follow the open-water testing. Cavitation occurs when the local pressure drops below the water vapor pressure (for that particular water temperature), causing “boiling” or bubble formation as the blades turn through the water. Figure 3 shows a test propeller in the circulating water channel. Note the cavitation trail from the blade tips, known appropriately as “tip cavitation.” The bubble formation and subsequent implosion causes damage to the propeller blade in the form of erosion corrosion, which looks like many tiny pock-marks in the material. A point of interest in this experiment is how the relatively soft epoxy of the composite material reacts to the destruction caused by cavitation. A reasonable hypothesis is that under normal operating conditions, a slowly rotating shaft – similar to that of the YP – a propeller blade (composite or metallic) would not rotate fast enough to cavitate. Furthermore, at higher speeds, a composite blade would deflect more at the tip, preventing the onset of cavitation.

Concepts and Materials

In the marine industry, nickel-aluminum-bronze is the standard material for many things, including propellers. There are several reasons for this, including its corrosion characteristics and anti-biofouling qualities. A nickel-aluminum-bronze propeller's role in the corrosion of the ship is reasonably simple. Galvanic corrosion is cathodically controlled, meaning that the extent of corrosion experienced is directly proportional to the amount of “electron taking” material present; the anode (in most cases, the steel hull and sacrificial anodes) begins to rust away. The primary cathode in the marine environment surrounding the hull is the NAB propeller. It does not corrode itself; however, it will cause significant steel plating rust and wastage of the sacrificial anodes. Reducing the amount cathodic material, such as NAB, could spawn significant savings in the millions of dollars per year the U.S. Navy spends on corrosion damage.

In the last few decades the loads on propellers have become less ambiguous. With the advent of computational fluid dynamics (CFD), using lifting surface and panel computer codes, the pressure distributions have been determined with more certainty. In some cases, it appears that the designs are conservative, as the factors of safety often appear higher than one might expect. There remains significant uncertainty in the fabrication of the propeller itself, but the allowable design stress remains approximately 12,000 psi. While the yield strength for NAB is dramatically higher, giving comfortable factors of safety well above two, the casting process often yields lower strength properties. Another significant drawback is the high cost of manufacturing a propeller from isotropic materials, specifically the hand-finishing and balancing. Though computer-aided-machining has substantially decreased the amount of time and money spent on producing the blades, a large amount of resources are spent on the final processes.

Nickel-aluminum-bronze is a well-understood material for modern-day propellers. For

instance, current submarine propeller designs have very advanced geometries yet they use traditional materials. One of the primary benefits of using nickel-aluminum-bronze is that the understanding of the metal itself compensates for greater misunderstanding in the loads experienced by the propeller. So why switch from a tried-and-true material such as nickel-aluminum-bronze to something much more experimental such as a fiber reinforced composite? The answer is that improved capability may be achieved through the advancement of material technology.

Knowledge of fiber reinforced composites was crucial to the design of this modified propeller. R.A. Higgins in his Properties of Engineering Materials, described fiber reinforced composites as a combination of a resin with fibers of some type.⁷ The project used carbon fibers woven together in a cloth format, oriented at angles of zero and ninety degrees to the reference axis. Its favorable stiffness and strength properties contributed to the selection of carbon as the propeller material. Since the precise loads that the propeller blades will experience are often unknown, the fibers must be angled several different ways, with the majority being oriented parallel to the loads most likely imposed due to the high bending moments. Since a propeller blade is very similar to a loaded cantilever beam, most of the fibers were oriented in the zero-degree configuration, which extends radially from the hub.

Encapsulation

In response to the need to lower costs in propeller manufacturing, personnel at the Naval Surface Warfare Center -- Carderock Division developed the idea of encapsulation. The concept began with the encapsulation of a rudder and skeg, and later progressed to a propeller for the Naval Academy Yard Patrol craft. The intent behind using an encapsulant on these objects was primarily to lower cost of fabrication. In using a polyurethane material – specifically Versalink –

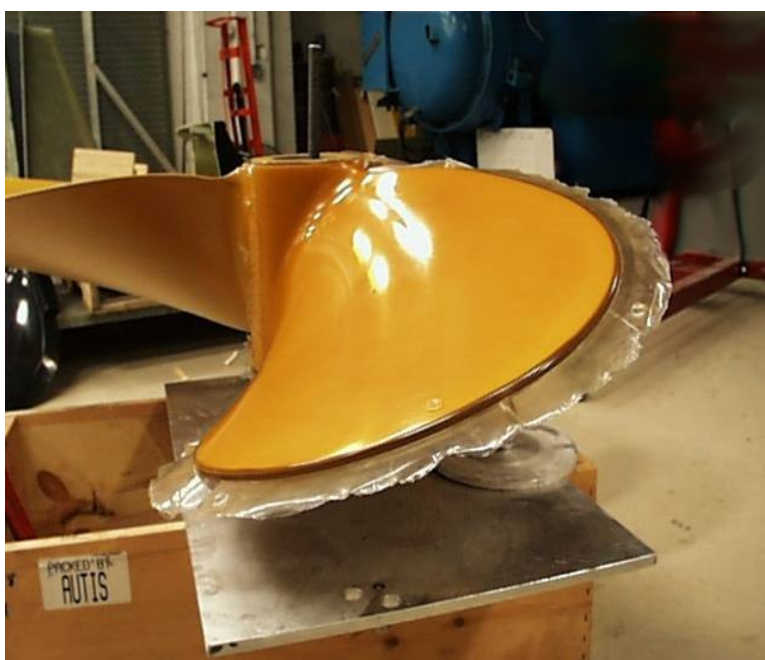


Figure 4 – Encapsulated Propeller

one could create a hydrodynamically smooth surface without the more intense metalworking required to finish a nickel-aluminum-bronze propeller. The core of the propeller, for instance, is almost the exact same dimension as the traditional propeller. Instead of a smooth metal skin on the outside surface, there is a layer approximately one-eighth to one-quarter of an inch thick made of a polyurea-based resin. The inner core is not machined to nearly as fine a specification as a typical propeller designated for ship use. In some respect, the added roughness aids in binding the polyurethane to the metal surface. As part of the overall propeller testing plan, the encapsulated propellers were installed and studied on YP677.

one could create a hydrodynamically smooth surface without the more intense metalworking required to finish a nickel-aluminum-bronze propeller. The core of the propeller, for instance, is almost the exact same dimension as the traditional propeller. Instead of a smooth metal skin on the outside surface, there is a layer

The process of creating an encapsulated propeller is reasonably simple. The resin must adhere to the surface, so the metal must first be prepared by sanding and application of primer material. A previously fabricated mold is then placed around the blade. This mold (seen in Figure 6) creates the spacing for the layer of polyurethane material. Some uncertainty is introduced, since it is rather difficult to create uniform spacing.



Figure 5 – Starboard Encapsulated Propeller

There are areas visible on the encapsulated propellers where the polyurethane layer is measurably thicker than other places. It is reasonable to estimate, however, that the variance is not much more than one eighth of an inch over the

Figure 6 – YP Prop Mold



entire blade. The area of largest uncertainty was around the hub, where fitting the mold was exceptionally difficult. Figure 4 shows a YP propeller right before the excess encapsulation

material is trimmed from the edges while Figure 5 shows the final product mounted on YP677.

David Owen and his team at Naval Surface Warfare Center -- Carderock Division conducted numerous tests on the durability of the Versalink polyurethane material in the marine environment. Tests such as the peel test, as well as various impact tests, indicated that the polyurea resin compound was as formidable as nickel-aluminum-bronze. The question that remains to be seen is the long-term durability of the material in the wider variety of water conditions experienced by a propeller – especially cavitation.

Composite Materials

Composite material engineering is similar in some fundamental ways to engineering with isotropic materials. There is a modulus of elasticity (or measure of stiffness), there is some degree of Poisson's Effect (the conservation of volume in a material, i.e. – the increase in width as a material is compressed), and there is also an upper stress boundary a material can withstand before failure. But this is where most of the similarities end. Composite materials are anisotropic, meaning that material properties can (and often do) vary in the xy -, yz -, and xz - planar directions. Therefore, unlike steel, aluminum, and other metals, the modulus of elasticity is not constant in all directions, nor does it deform under stress in the same manner.

Additionally, composite materials do not generally fail in the same manner as those with isotropic properties. Much depends on the type of loads as well as the actual material fabrication. To begin the design process concerning composite materials, one must first understand some of the methods to design, a few of the basic failure modes and changes in material properties, and an understanding of what factors can affect damage tolerance.

There are two primary ways to engineer a composite structure. One could design it like an isotropic structure using factors of safety and material properties such as the modulus of elasticity and yield stress. Though these properties vary from plane to plane, one could account for such changes using matrix mathematics or by blending the properties into a single modulus of elasticity. This method tends to yield more conservative designs, as it relies on a large factor of safety. For instance, if the allowable factor of safety for a deck hatch constructed from an isotropic material is 2.3, a similar deck hatch of fiber-reinforced composite could be twice or three times as high, due to variation in the material or fabrication method. The variation is not in the material itself; carbon fiber, for example, has relatively consistent properties, as well as the

laminating epoxy. The inconsistency, then, comes largely from the construction of the material. Much depends on the component's fabrication process; whether there are areas of microscopic air entrainment, contaminants present between the layers where the chemical bonds could not form correctly, and appropriate fiber orientation for the design loads are all reasonable questions that must be addressed. Two of those factors: the contaminants and the presence of air bubbles are very difficult to prevent.

The benefits of using composite materials might be unclear. When engineered correctly, they are often as strong, if not stronger, than isotropic pieces and they are generally much lighter. If weight is the primary driving factor behind a design, the extra hours invested in composite engineering is time well spent. If a structure is to be its lightest, though, the properties method is not the most efficient way to design. Instead, one could use classical lamination theory and probability and statistics to design a structure.

Unlike isotropic materials which have a single modulus of elasticity, classical laminate theory takes into account the varying elastic properties of a material based on the direction of deflection. A piece of 2"x4" lumber behaves differently when loaded parallel to the wood grain versus perpendicular to the grain. The multiple elastic constants are related in matrix format. So, matrix math is then used to solve for strain and stress.

Probabilistic structural analysis, as it is called, finds the most likely value for a given constraint, such as deflection, bending moment, material properties, etc. by running multiple calculations with varied "primary variables" such as length, stiffness, or thickness in a process known as a Direct Monte Carlo Simulation.⁸ The results of the simulations are combined to form a roughly normal distribution. For instance, when speaking of the loads placed on a structure, there is a small portion of the time that the "worst-case scenario" actually occurs. With

traditional “working stress” design, the structure is engineered for exactly that case.

Probabilistic design allows the engineer to develop a structure closer to the actual acceptable values of stress, without being overly conservative or assuming that the structure will never meet a given load. This risk analysis process provides two primary pieces of information: the reliability of the structure and the primary variable affecting that reliability.⁹ Additionally, such analysis helps to predict and prevent fatigue related failures, as it takes those factors into account as well.¹⁰

Depending on the purpose of the engineering project, either method would work well. For example, if one were to build a bridge, the working stress method would probably be more than adequate. There would be some parts that are too conservative, but the cost of that over-engineering might outweigh the cost of the probabilistic analysis beforehand. This is especially true in engineering with isotropic materials. With anisotropic materials, like fiber reinforced composites, the variation in fabrication and material properties is often too great to ignore; so, probabilistic analysis is preferred. Variables of primary concern include: the materials used; poor fiber alignment; structural ratios comparing fiber and epoxy volumes; and, ply/fiber orientation and thickness.¹¹ These factors, especially if combined, can create a drastically different material than what is intended. The engineer should then consider the probabilities of each variable occurring and to what intensity they occur. For instance, is the fabrication company known for making inconsistent materials? If so, how inconsistent are they and in what manner? In addition to a more efficient design, the engineer is better able to identify the decrease in fiber strength after fabrication compared to the new, unprocessed fibers (in situ vs. pristine strength).¹² While probabilistic design is preferred, it requires a large amount of historical data to produce improved results. Before a probabilistic design is undertaken, data

pertaining to these variables must be compiled and analyzed to produce reliable probability distributions.

Part of the difficulty in composites engineering is the relative uncertainty of the materials in question. With steel, the properties are similar from girder to girder, as well as from plane to plane. Composites are not so similar in that regard, and require special treatment in order to construct a safe, reliable structure. The concern is in knowing how to find and predict the various failure modes of these composite structures.

A caveat of composite materials is the change in strength due to fabrication, which is a driving force behind the need for probabilistic design. But, once the structure is in use there could also be a change in strength due to exposure of the fiber to heat or chemicals through matrix cracks.¹³ This phenomenon is of special interest for composite materials exposed to the marine environment for a prolonged period of time. If strength loss does result, determining how the life cycle is shortened is vital to developing a maintenance/replacement plan.

Aside from inherent abnormalities due to fabrication, a designer must concern himself with another failure mode: cracking. Cracking occurs in two primary ways: matrix cracking and delamination. Both modes of cracking are rather difficult to predict, especially since they often start on the elemental level. Matrix cracking tends to occur due to a microscopic stress redistribution, or micro-cracking.¹⁴ Hidden beneath the layers of composite cloth and epoxy, micro-cracking can begin with few visible indications. A study by Kenneth Reifsnider found that stress redistribution is critical under uniform loading conditions, but is even more important when the loading is cyclical, like a propeller, in nature.¹⁵ His study, though, focused on axial loading as opposed to bending moments, which raises the question whether there is a significant difference between cyclical axial loading and cyclical bending moments. Perhaps it is even more

crucial with cyclical bending moments, as the loading on the fiber level would range from tensile to compressive stresses and back again as the structural member undergoes each cycle.

The next step in the damage progression once the matrix crack begins to form is important. In a material like steel, a crack generally propagates to infinity (depending largely on the member's physical characteristics), but little can stop a crack once it begins. In composite materials, crack propagation has a general direction: away from matrix rich regions toward the fibers themselves.¹⁶ If the fibers are above the necessary strength level to withstand the applied load, then the crack propagation could cease.

This sort of cracking, oftentimes on the interior of the structure, is difficult to detect except by a non-destructive means, such as x-ray or ultrasonic analysis. Eventually this sort of micro-cracking failure would cause global failure of the structure. While micro-cracking is generally undesirable in marine structures due to increased moisture absorption, there are some structures where such cracking does not constitute failure. As part of the probabilistic analysis, one would need to determine if the loss of strength would lead to failure. If that analysis proves that slow growing cracks are not sufficient to cause structural failure, then costly inspection methods are unnecessary. So the question becomes what constitutes structural failure. For most components or full structures, failure is the point at which it is unable to withstand the design loads placed upon it. With this specific failure mode, the cracks could grow slowly enough not to affect the load bearing properties of the component. By the same token, they could be the turning point for a given structure; it functions properly until these micro-cracks begin to form, then failure occurs. Much depends on the nature of the composite material and the purpose of the design.

The other type of cracking failure is called delamination. While the matrix cracking

could extend farther in the planar direction or remain as a hairline fracture, delamination continues across much, if not all, of the given plane between layers of fiber. There are several direct causes of delamination, which include poor fiber matrix or ply adhesion, epoxy-rich regions, and low velocity impact.¹⁷ If the composite material were used in a marine environment, be it as a rudder, hull, or propeller, low velocity impact would be of significant concern. Delamination may or may not turn into complete structural failure, but the nature of this sort of weakness leads itself into structural failure. It is a relatively large area where the ply of carbon, or other fiber fabric, has become separated from the resin matrix or the adjacent ply. When placed under a load some percentage lower than the intact failure load, the delamination area will increase. Ultimate failure is the point where the delamination width is wide enough to preclude the component from withstanding its design load. Note that this sort of failure may occur under both static and cyclic load conditions, both of which are studied by using the double cantilever beam, end notched fracture, and mixed mode bending experiments.¹⁸

One might conclude that worse delamination might occur under cyclic loading. This particular study does not indicate whether cyclic or static loading is worse than the other. Using a stronger or more durable resin could mediate delamination and prevent its destructive effects. If the resin is forgiving enough to flex with the fibers, delamination would not likely occur, especially if there were no more than minor fabrication imperfections. Part of the greatest benefit of composite material engineering is that each material can be engineered differently and for a different purpose, so the stiffness characteristics may be changed. The composition of the structure may be manipulated such that delamination may not occur. Fabrication uncertainty cannot be entirely eliminated by design, but the effects thereof can be significantly limited.

Any structural component, be it a steel bracket or a carbon-epoxy frame, is subject to

various types of damage loading. A damage load could be some sort of impact, fatigue, or periodic excessive loading. While the effects of fatigue and excessive loading are often limited by design, impact loading is often unpredictable. A component could complete its life cycle without experiencing an impact load. At the same time, a similar piece could only make it through a quarter of its service life due to severe impact damage. Much depends on probability and the environment in which the component operates. Impact is usually characterized by the speed at which it occurs, ranging from low to ultra-high velocity. In the marine environment, with the exception of warship ballistics, impact generally occurs at low velocity on the order of magnitude of tens of meters per second. Each structure should be built with some degree of damage resistance, the degree varying according to the purpose and situation.

One might question which component of the fiber-epoxy material is most crucial to damage resistance. While it might depend a great deal on the combination of the two, the fibers tend to respond in a linear elastic manner. In other words, they are inherently more resistant to damage simply because they have the capability to respond, much like a rubber band is more resistant to impact than a glass plate. The damage variable then becomes the epoxy matrix. More often than not, the resin is a hard, brittle material. It is very capable of holding plies of carbon or Kevlar fibers in place, but is less than ductile in its own right. So, to create a more damage tolerant component, the more critical aspect is choosing a better resin than finding a better fiber.¹⁹

When the impact loading occurs, it can cause various levels of damage. Additionally, the level may be raised by subsequent, less powerful impacts. These damage levels begin with matrix cracking, then to crack propagation leading to interfacial debonding, to delamination, fiber fracture, and finally perforation.²⁰ The damage tolerance of a material or structure is

classified in one of two ways: if the structure is capable of withstanding a higher load without damage progression; or, if the structure is capable of withstanding its design loads once damage has already occurred. Seldom is a structure designed to meet only one or the other criteria. The overriding condition is accomplishing its initial set of design criteria. Designing it such that it can withstand more damage and still function properly is beneficial, though sometimes costly, to produce.

Of the different damage levels, perhaps the most serious is delamination. As it was defined previously, it is ply separation in a fiber-epoxy material. In most cases, the residual strength of the component is significantly decreased once delamination occurs. Such strength degradation prohibits the component from fulfilling its design parameters, thus constituting structural failure. While the other damage levels before delamination can reduce residual strength, delamination might be the most significant.

If a composite structure is struck with an object, the resultant damage is a product of the particulars of the collision. The object's mass, speed, shape, direction, and hardness are all influential. In a subsurface marine environment, collisions are generally low speed with hard objects, like rocks, sunken trees, and other submerged debris. Again, the area most susceptible to damage is not the fibers, though they are subject to fracture in the collision. But before fiber fracture occurs, delamination will take place. When diagnosing the amount of damage to the component, the area of delamination is of primary concern. If the damage level is high, the area of delamination is likewise high. In this case as well, the fibers are not the component responsible for delamination. Instead, it is the resin matrix and the bonds that it forms with the plies that determine to what extent the delamination spreads. Delamination areas that result from a collision differ from resin to resin; at times dependent on how the resin is cured as well as the

chemical interaction between it and the fibers. Another driving factor is whether it is a thermoset or thermoplastic resin.²¹ Thermoplastic resins generally produce smaller delamination areas after impact, but may not be suitable for certain applications.

When designing a composite structure, it is generally beneficial to utilize probabilistic tactics in order to account for material variability, if the necessary data is available. By determining the probability of the highest load to the weakest material, one is able to start the design process. This process tends to be more reliable than working stress methods, especially if the design loads, environment, and material are not well understood. Additionally, it helps to determine which material characteristics are most influential in a given design. When speaking of failure modes, note that the resin matrix affects to what degree failure occurs; whether it is matrix cracking or delamination. Combining the results of probabilistic analysis and the types of epoxy available, the amount of damage tolerance is estimated. Probability also plays a major role in what defines failure and how long the life cycle of a component should be. While the type of fiber for a given application is important, the type of loading and probability of impact dictates the type of resin that should be used.

Much depends on the type of composite materials that are implemented in the various sorts of environments, but there are certain, somewhat universal properties of fiber reinforced composites. For instance, the matrix is generally the first point of failure, then the fibers (unless the load experienced is significantly higher than the design specifications, in which case both fail almost simultaneously). Also a large amount of variation is experienced by using the same materials in different configurations, contributing to the wide versatility of composites. Understanding how a composite component will fail and knowing how such failure might be prevented is crucial to designing a strong, reliable, and durable structure.

Propeller Blade and Hub Fabrication

The process of designing the composite bladed propeller had several steps, many of which relied on newer, less utilized technologies. While probabilistic design would have proven beneficial, the lack of detailed data available meant the more reasonable method was to increase the factor of safety margin. The first step was the design of the hub (refer to Figure 1); a crucial piece that -- if designed poorly -- could cause catastrophic propeller failure. Two primary designs were first considered. The first was similar to the design used by the English company QinetiQ on board the experimental ship *Triton*. In this particular design, the composite blade would slide over a NAB nub and be pinned in place. At first glance, this design raises several concerns; the most obvious being the stress concentrations formed due to the pins. Additionally, the metal inclusion within a composite structure could possibly cause cracks to form at the metal/composite interface. The flexing of the propeller during its use would only force these cracks to propagate, possibly leading to eventual blade failure.

The alternative design is that used by the AIR Corporation of Germany. Their idea uses a purely mechanical dovetail hub-blade interaction. One of the key advantages is the propeller's segmentation, where the blade is a piece entirely to itself, leading from within the outer hub radius to the propeller tip. More importantly, there is no metal inclusion nor any holes drilled into the composite blade. Furthermore, if the propeller were to strike debris while in use causing damage to the blade that might require repair or replacement, it could potentially be replaced underwater with little or no damage to the hub itself. The primary drawback to this design, however, is the more complex design process, analysis, and manufacturing of the pieces involved.

For several reasons, from better fiber continuity to fewer stress concentrations, the dovetail design was selected for this project. While the British design shows definite promise, and has been used on the HMS *Triton*, it seemed wiser to put forth more effort in creating a mechanical system rather than trying to solve more complex stress concentration issues involving a composite material. For a three bladed propeller such as that of the Yard Patrol

Figure 7 – Dovetail Hub Acrylic Model



Craft, one must be careful of taking too much material out of the hub to make room for the composite dovetail. Also, the Yard Patrol propeller is rather thick at the root section; therefore, the dovetail must be thick as well. This is just the first of many trade-offs made during the hub design process. Figure 7 illustrates the residual material concern in the form of an acrylic model.

Using the Rhinoceros 3-D modeling program, an iterative design was initiated. Several different approaches were undertaken in attempt to satisfy the need for sufficient propeller root thickness as well as an ample amount of remaining nickel-aluminum-bronze in the hub. Once a

version of the design was finalized and checked with finite element analysis, a scale model was fabricated using the stereolithography rapid prototype machine (more simply known as the three dimensional printer). While the prototype machine used in the Model Shop costs over one hundred dollars per pound for each part made, it was still far cheaper and significantly faster than traditional methods of prototype manufacturing.

In addition to a scale hub model, a complementary small scale blade was designed in Rhinoceros 3-D and produced using the rapid prototype machine. Once the hub and blade design were proven with small models, a full scale Yard Patrol propeller blade was made out of epoxy by Mr. Paco Rodriguez at the Naval Surface Warfare Center -- Carderock Division using their much larger rapid prototyping machine. This blade was used as a plug to make the fiberglass molds.

Methods of Experimentation

Coupon Testing

Coupon testing is a method of fabricating a small composite material test section and evaluating its material properties. Also in this case, the strain gages laminated between its plies. There were several goals for this coupon test: the first being the necessity of showing that this sort of instrumentation was a logical process. Secondly, it was important to study the causes of energy loss within the fiber optic material for designing an embedded strain gage system used on an actual propeller (see “Fiber Optic Strain Gaging” subsection for further information). A third objective was to determine the strain gage orientation within the laminate. A piece of fiber optic material is very similar in appearance to a larger diameter strand of fiberglass; and like fiberglass, it becomes transparent when covered in epoxy. It is crucial for all types of strain gages to know the exact orientation. Without knowing the strain gages' positions and orientations, the determination of the material strain and stress is impossible. Finally, the strain gage information could be used to confirm composite material analysis in the finite element program. Such confirmation on a small sample helps to determine problems in the solution formulation used by the finite element analysis code. If problems exist for a small sample, it will likely worsen exponentially with a more complex geometry such as a propeller blade.

Full-Scale Testing

Another method of experimentation was full scale testing of the Yard Patrol craft, YP677. Three specific batteries of tests were laid-out: the baseline NAB tests; the encapsulated propeller tests; and, finally the composite versus NAB tests. To collect information from such tests, extensive data acquisition instrumentation was required. Mr. Dave Burroughs, an employee of Naval Surface Warfare Center -- Carderock Division, played an integral role in the installation of the required gages. Strain gages were placed on each shaft to determine the propeller torque, photo-optic sensors were installed to read each shaft's revolutions per minute, and a serial feed was taken from the shipboard GPS for speed over ground and position measurements. The objective of these tests was to develop performance baselines and to test the propellers in the actual in-service conditions. Data was collected for several different cases, from straight line runs to full circles to the harshest of all conditions, the full-speed, emergency stop.

Fiber Optic Strain Gaging

As previously mentioned, the use of fiber optic strain gaging technology in a composite bladed propeller would prove useful in better understanding propeller design, as well as the effects of the fluid conditions experienced by the blade. Before this technology may be used, one should prove its feasibility. The first step in this process was the analysis of a test coupon. There were several strands of fiber optic material laminated within the test coupon, each bent to a different radius. The objective was to determine the smallest usable radius where the light could travel without significant energy loss. These strands were plain glass without strain gages. One strand, which ran with the fiber bias, had a refraction grating strain gage included. The grating's purpose was twofold: to provide strain information when in a loaded condition and to develop a method of marking the gage's orientation. Using a Sharpie marker on the gage's protective coating, a distinct red mark was visible. Weaving the fiber optic strands into the carbon fabric was straightforward; however, the fiber-exit was substantially more difficult. The hurdle was not in leaving bare fibers outside of the laminate but rather considering the ramifications of having to machine the edges. If the fiber optic technology were used in a propeller, the fiber ends would probably exit through a machined edge. Finding a way to route these fibers out of the laminate while preventing machine damage was critical to the test coupon experiment. Like many other forms of experimentation, it is far cheaper to lose one gage in a coupon than to lose several gages in the final propeller.

The intent of the test coupon was to confirm results yielded by the finite element program. Learning the stress analysis options, different types of elements and their uses, as well as interpreting composite analysis results were important skills to acquire before moving on to more complex analysis. Appendix A clarifies the experimentation process used for this portion

of the project. Exposing the test coupon to a gravity load and measuring the strain from the gage would serve as a good comparison to the finite element results. Additionally, readings from conventional resistor-type strain gages were part of the additional verification procedure.

Weaving the fiber can be done easily, but routing the ends of the fiber from the laminate is a success-failure sort of operation where there may be only one opportunity for success. An additional difficulty for a propeller is that it rotates underwater. The rotating action alone may be enough to destroy the fibers, while additional complications would result from the added hydrodynamic resistance on the fibers. Moreover, a data collection unit capable of receiving the fiber optic signal from rotating strands requires significant development. Another concern is that if the fiber is laminated too close to the surface of the propeller, it may be exposed after the surface is worn away by cavitation. If it is not completely separated from the laminate, further erosion could fracture the fiber or the water flow over the small, exposed bump could be enough to lift the strand from the surface and destroy it.

The AIR corporation had made parallel attempts at utilizing the embedded strain gage technology. Their efforts produced similar conclusions, highlighting the fiber exit point as the weak link. Fiber optics work on the principle of sent and received light. Ideally, a light of a given wavelength would enter at one fiber end exit through the other exposed end. However, these gages have the ability to send and receive information through the same end. In practice, a signal is sent through the fiber in the form of a light of a specific wavelength. The light then passes through a diffraction grating that changes its characteristics with the amount of strain it experiences. The altered signal has a wavelength proportionally smaller than the input signal, indicating the amount of strain experienced at that section of the material. As many strain gage gratings can be created on a single fiber strand, this technology offers a significantly more

compact arrangement than traditional resistor gages. Additionally, as the fiber is inert, the gage will not corrode like the copper-based resistor gages.

The first attempt at coupon fabrication had its difficulties. A piece of plywood was used as a base underneath the laminate. As it was curing in the hot summer sun, the heat caused the thin strip of plywood to warp. Likewise, the laminate cured in a curved position, leaving indeterminate residual stresses in the fibers. Even in an unloaded condition, the strain gage would read a certain amount of strain. The difficulty lies in determining the zero point. If the calibration of the fiber optic gage was not so sensitive to changes in temperature, determining the amount of residual stress would be relatively straightforward. Additionally, load application to a warped test section became difficult. The laminated test piece was curved such that adding weight at any specific point was difficult to do with precision. In addition to the plywood warping, the laminate was only a few plies thick. Therefore, it would have been difficult to apply loads without passing into the nonlinear stress zone. The first round of experimentation yielded improvements for the following coupon test iterations; specifically, creating a thicker laminate cured on a more rigid surface. The first attempt also served as an introduction to practical composite lamination.

A second effort was made by using several plies of carbon laminated on a granite tabletop. Several plain strands of fiber optic material and a single gage were woven into the first layer of carbon fabric for the energy loss study. This time, another difficulty arose. To route the fiber out of the laminate away from the “machined edge,” the strand of glass had to exit almost vertically, causing a kink. A tight bend with a very small radius contributes to energy loss that cannot be quantified easily or consistently. A catastrophic mistake was also made by placing a layer of Peel-Ply on the laminate surface. Peel-Ply is a porous sheeting material that does not

adhere to epoxy. It is often used as a barrier between an epoxy sponge material and the laminate in a vacuum bag set-up. Ideally the Peel-Ply could be removed cleanly; however, the epoxy stuck well enough to both the fiber and the Peel-Ply that, when removed, the Peel-Ply sheared the fiber optic ends at the surface of the laminate.

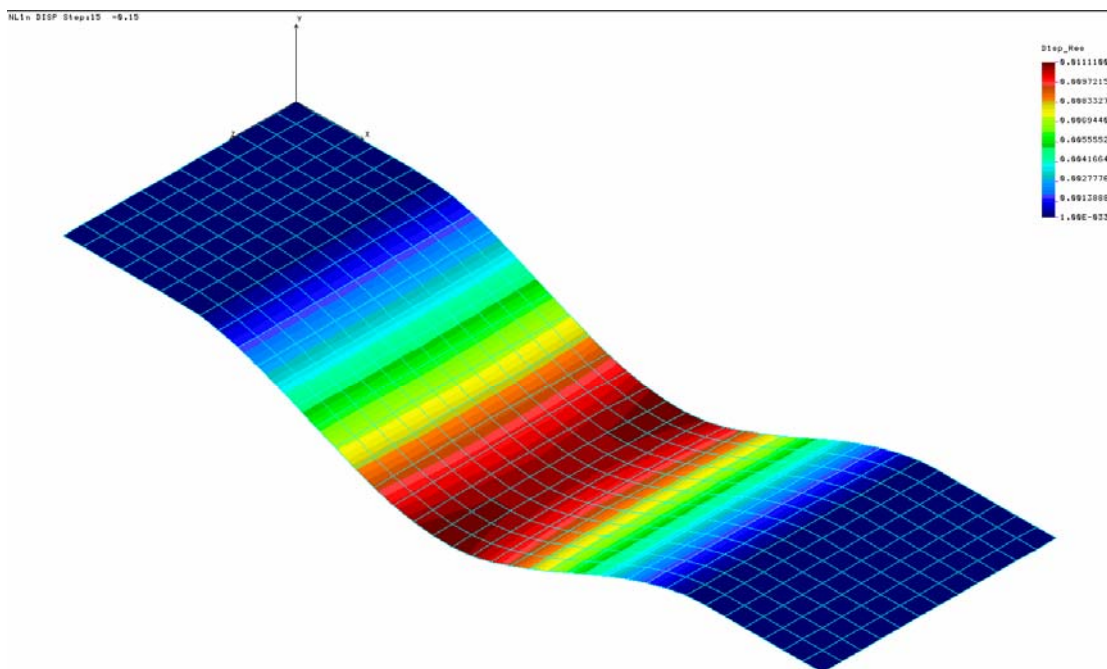


Figure 8 – Test Coupon Displacement Plot

Since no strand -- and specifically the strain gage strand -- failed to survive the lamination process, loading the test coupon with any sort of weight would yield no measurable data. Mounting the fiber optic gages on the surface along with the resistor-type gage was a possibility, but the larger issue environmental issues between the test coupon and the propeller remained. Leaving the fiber optic gage on a propeller exposed to the environment may only work for a short time, if at all. Additionally, if the gage were embedded, bringing the fiber ends out of the laminate remains almost impossible to do effectively. Figure 8 is representative of the test coupon's displacement reaction to the gravity load if the experimentation was fully executed.

While this experimentation occurred, the AIR Corporation was having similar troubles on

their own composite blades. The primary concern remained getting the fiber ends through the surface of the blade without damage during the finishing processes. The conclusions to both lines of experimentation, especially in light of this project, are that embedded strain gage technology has significant promise, but the technology must progress further before it can be utilized with a propeller. In particular, the frailty of the fibers is cause for concern in harsh environmental situations. Still foremost on the list of difficulties is the fiber-exit from the laminate. If it is through the surface of the blade, the fiber will experience the effects of flow exposure. At the same time, if the exit is through the dovetail into the hub, sliding the blade in or out and machining the dovetail, would be nearly impossible without shearing the fibers at the laminate surface. Once the technological state of the embedded fiber optic strain gages advances to the point it can be used more efficiently in the marine environment, it will become an invaluable asset to better understanding the stresses experienced by a propeller blade as well as for improving the design of composite blades. Given the difficulties encountered, further fiber optics research was curtailed in this project.

Dovetail Design and Load Generation

Dovetail Design

The starting point for the composite bladed propeller design was the nickel-aluminum-bronze hub. Utilizing three-dimensional computer modeling tools, developing a conceptual design allowed numerous iterations at minimal cost. Much of the time spent was in learning the Rhinoceros 3-D program and how to work with the various surface/volume commands. The conceptualized hub involved cutting three twisting dovetails along the outer edge of a cylinder. The incorporation of corner fillets, helical cut paths, and the tapered dovetail made developing the hub a challenging task.

Using the modeling program, an iterative design process was undertaken. Creating a general dovetail section to prove its applicability began the design spiral. With each passing iteration, the depth of the dovetail, wedge angles, rate of helical rotation, and fillet radii were changed to yield geometry with strong fiber continuity and lack of stress concentration areas. The first model had narrow, shallow cuts for the dovetail slots to prove that the modeling program was capable of creating sealed volumes – a requirement of most rapid prototyping methods. The second revision had incorrect wedge angle which prevented the blade from sliding into the hub and remaining fixed.

Wedge angles proved difficult to change without completely recreating the hub. Too acute an angle would cause fiber kinking in the manufacturing process, while too shallow an angle would increase the risk of the blade not being held securely in place. An algorithm was written to generate points for different wedge angles. When used with a RhinoScript (a text file with specifically ordered Rhinoceros-3D commands), the amount of time needed for a new iteration was decreased by a factor of ten. Small changes were made in the depth of the dovetail,

position of the edges compared to the blade surfaces, and wedge angles to later yield the final version. Extra distance between the blade surface and the dovetail edge would cause fiber discontinuity, as well as extra plies of carbon required in the dovetail and less bronze in the hub. Once the twists and angles were satisfactory (wedge angles of less than fifteen degrees), the volume could be used both as the cutting tool for the hub and the complementary male dovetail piece for the blade. The dovetail piece then had to be mated to the complex blade geometry.

Personnel at the Naval Surface Warfare Center -- Carderock Division, specifically Mr. Michael Harshaw, possess a blade measurement, digitization, and surface rendering capability. Using a full-scale nickel-aluminum-bronze Yard Patrol propeller, point measurements were taken at fifty-eight points on fifty-two radii of a single blade. Each point was assigned an individual x-y-z coordinate. When imported into the Rhinoceros program, the coordinates created what is called a "point cloud." Connecting the points along each of the radii yielded an airfoil shape. From these curves, it was possible to create a surface connecting all the cross-sectional shapes, thus rendering the first revision of the blade surface. The leading and trailing edges were often difficult to cover with a standard surface and required approximation to complete the blade geometry. Additionally, the root section and hub fillet dimensions were difficult to measure and often produced unfair, inaccurate surfaces in the model.

The faired geometric characteristics of the blade paired with NSWCCD's propeller design program produced a much smoother surface file. The root section of the faired blade extended farther toward the center of the propeller, eliminating the hub fillet and creating sufficient volume overlap for the Rhinoceros program to join the blade with the previously designed dovetail. Once the blade was joined with the dovetail and the hub had been completed, a small scale version of the entire design was sent to the three-dimensional rapid prototyping machine,

resulting in a model like that in Figure 9. Each of these small models costs less than \$100, but their importance was immeasurable. The small changes made at each step were inspired by the physical characteristics of the preceding small model. It was easier to see the hub-blade interaction in the form of a physical model instead of analyzing the images on a computer screen.

Not only were the rapid prototypes cost efficient, they also saved valuable time during business hours. A model could be finalized on the computer screen, taken to the three-dimensional printer interface, and a small scale model would be ready for use by the next

Figure 9 – Hub and Blade Model



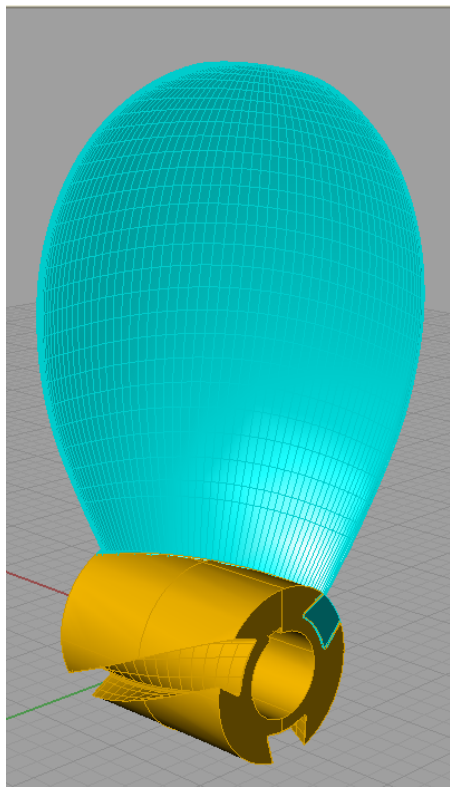
morning. Manufacturing such pieces using conventional machining methods may have taken weeks as opposed to the few hours required by the rapid prototype machine.

While numerous iterations led to the desired design, a great deal was also learned about three-dimensional modeling program, as well as effective use of the rapid prototype machine. The end result was a tangible, physical model which decreased the uncertainty of relying purely on a computerized conceptual drawing. Figure 10 shows the final computer rendition of the blade/hub apparatus.

With experience, three-dimensional modeling became a more straightforward and efficient process, resulting in the creation of the RhinoScript algorithm for dovetail design mentioned earlier. While this program would benefit from minor improvements, it reduced the

amount of time per design iteration from approximately three hours to thirty minutes. As it currently reads in Appendix B, the dovetail design program does require user familiarity with the code, as well as experience with the modeling program. An ideal end-state for this program -- and possibly the basis for further research and development -- is a more efficient, streamlined code with an improved user interface and greater flexibility to make a universal method

Figure 10 – Blade/Hub Rendering



applicable to a variety of propeller designs. Since each dovetail design involves complex curves and tight precision, a more accurate design would result from letting the computer calculate various point and curve locations instead of relying on user-definition.

Load Generation

The blade's geometry file was the beginning step of the three-step analysis process. The other two phases were the load generation and finite element analysis. To produce a well-designed structure, it is important to understand the loads that the structure will encounter. For instance, if one were to design a fence post in an area where the maximum wind is above sixty knots, it would be measurably stiffer than a fence post designed for an area with a maximum wind speed of less than twenty knots.

Society sees both ends of the engineering spectrum, from relatively risky designs for space shuttle components, to the more conservative designs of automobiles with reinforced body panels, airbags, and stiffened frames. There are two primary motivators for conservative design: the first being a requirement of exceptional safety (for example: commercial airliners) and the other the presence of load uncertainty. A relative scale of "conservativeness" is known as the factor safety.

In the case of propeller design, the loads can be calculated for steady state conditions with acceptable accuracy. Thrust characteristic programs at NSWCCD produced a pressure distribution for the Yard Patrol blade. The first step was taking the faired propeller geometry and inputting it into a lifting surface code. The lifting surface method is one of the more advanced, yet traditional, methods of designing a propeller. In this particular case, the design already existed, but the pressure distribution over the blade surface was unknown. Design parameters and coefficients produced by the lifting surface code were then sent to a panel code. The panel code is one of the most advanced propeller design algorithms in existence today and yields some of the most accurate results. The output from this program could be imported into a program written by Mr. Thad Michael of NSWCCD to translate the pressure distribution

calculated by the panel code into information useful to the finite element analysis program.

The end result of his program was a NASTRAN FEA file complete with elements based on the input geometry and a pressure distribution developed from the panel design calculations.

NASTRAN is the finite element program of choice for NSWCCD, while this project used COSMOS/M. The final step was converting the NASTRAN file to a COSMOS/M file, which is easily done with the finite element translator included with COSMOS/M.

There were several assumptions made in the load generation process. First of all, as the panel code does not take into account for thrust reduction due to cavitation. As mentioned earlier, cavitation is bubble formation on the blade surface due to exceptionally low pressure. Several factors affect cavitation: speed of propeller rotation; blade shape; water temperature; depth of propeller submergence; and, the relative ability for the propeller to draw air from the surface in a process known as ventilation.

When a propeller cavitates, no lift is produced where the cavitation occurs. Perhaps this can be thought of as the limit of the propeller's effectiveness. More thrust is produced as the RPM increases, but the rate of thrust increase is much slower than that before cavitation inception. The design case for this particular project is the Yard Patrol craft in an ahead full condition with a speed of twelve and one half knots at 400 RPM. This makes two primary assumptions: that the installed engines are still capable of producing that much power and that the propellers are not cavitating. The first assumption is unlikely to be true; the second assumption is known to be false as the YP propeller begins to cavitate between ten and eleven knots, depending on the condition of the propellers and hull cleanliness.

The second key assumption concerning the load generation process is the code's elimination of unsteady forces. A propeller in the wake of a ship, specifically a ship with

pronounced struts, experiences a period of reduced water velocity downstream of the structures. With a lower velocity comes a smaller amount of lift when the propeller blade passes through the low speed zone. NSWCCD's panel code sees each blade as if it were experiencing uninterrupted flow, creating a maximum pressure distribution. The result of this assumption was a somewhat more conservative load case since the propeller seldom experiences completely uninterrupted flow.

For the propeller design codes to work effectively, the Yard Patrol craft's wake distribution was required. A wake distribution, or wake survey as it is often called, provides information as to the non-dimensional speed of the water through the propeller disk. The water's velocity through the fluid field along the ship's hull is some fraction less than the ship's speed through the water. Extensive research and development was done on the Yard Patrol craft at the Naval Academy both during its design phases and after its construction. At some point, it is likely that a wake survey was completed for one of the models. However, that report (if it existed) was washed away with the flooding of Hurricane Isabel last year. Instead, a survey done on a somewhat similar hull-form was adapted for the program. For even better accuracy, a wake survey of a more similar vessel would have been found, or another survey would have been done specifically for the YP. On the other hand, a wake survey experiment would have been difficult to accomplish given the post-Isabel state of the Naval Academy Hydrodynamics Laboratory. Regardless, the panel code dealt best with a more average survey. The distribution information used contributed to the more conservative pressure distribution as it had less flow obstruction than a Yard Patrol.

The combination of these factors yielded a more conservative load case. This is acceptable, partially because of incomplete information regarding the Yard Patrol craft, as well

as the need to back-solve from the propeller geometry. Additionally, it is beneficial to include a higher factor of safety when working with fiber reinforced composites, since the material properties of the fiber reinforced composite are not as consistently predictable as those of an isotropic material. The goal for this project was not to design an entirely new propeller, but rather to take an existing hydrodynamic design and apply a new structural design. The next step took the load condition based on the initial hydrodynamic design and determined a composite material strong enough to compare adequately with the nickel-aluminum-bronze structure.

One other consideration was the method of creating the finite element model from the calculated geometry and pressure distribution. On designs with greater amounts of skew, pitch, and rake as well as more complex leading and trailing edge designs, the propeller geometry is approximated as a six sided figure. This adjustment makes the model conform more completely to the finite element program's acceptable element geometry thresholds. It decreases accuracy by a negligibly low percentage. This loss of accuracy was of little concern for the Yard Patrol propeller, as the actual blade geometry lacked most of the "special" features that would lead to the creation of invalid elements or matrix singularities.

Finite Element Analysis

NAB Propellers

Once the load distribution was created, the final step was applying it to the blade geometry with the dovetail attachment and determining the stresses and corresponding factors of safety. The result of the NSWCCD finite element generation codes was a series of elements with an applied pressure field. Default boundary conditions, otherwise known as structural constraints, fixed the propeller in space around the perimeter of the root section. Not only is it very difficult to fix a point both in translation and rotation (as a fixed condition does), the composite blade will be constrained along the edges of the dovetail and not along the root section of the blade itself. Most propellers designed by at NSWCCD are to have a maximum combined stress of 12,000 pounds per square inch (psi). Final checks indicated that a nickel-aluminum-bronze YP blade confirmed this assumption. Initially, however, there was concern because the thrust from the blade seemed extraordinarily high.

The first thought was that the load distribution was incorrect, either because of poor control assumptions or flawed propeller geometry. In actuality, the error was not in the computational fluid dynamics analysis; it was in the construction and translation of the finite element model. One problem was the very high pressures, or very low pressures in some instances, along the edges where the fluid dynamics equations began to lose their validity. When the finite element model yielded results that were over 100 times too great for the von Mises combined stress, doubt was cast on the pressure calculation programs. Calculation assumptions and user-defined variables were checked and modified as needed, with no significant change in results.

Examination of the finite element model construction code indicated that several load

conditions were available, primarily the main pressure distribution and a distribution which included a viscous friction pressure component. This raised two issues with the COSMOS/M program, the first being the viscous pressure was defined tangential to each element. Some analysis codes are better at dealing with certain load cases and directions; COSMOS/M was not easily compatible with that direction. Additionally it was discovered that a very significant coefficient multiplier was excluded from initial computations. Thus, the viscous fluid friction terms which are usually very low were several hundred times too great. Also, the COSMOS/M program combined the load cases making the pressure distribution on the blade surfaces at least twice the correct value. Adding the increased viscous friction pressures yielded combined stress values for the NAB blade understandably outside of the expected range. The command list for the finite element program was changed to allow only one load case, without the viscous pressure component. Since viscous friction tends to be a minor factor, there was little hesitation about excluding it.

The ability to generate a valid pressure load had several contributing factors. First of all, the YP propeller has a simple geometry with small skew and rake angles. In fact, when looking at the propeller, it is very difficult to determine the leading edge from the trailing edge. Often times, it can only be done by physically touching the blade or reading the information inscribed on the hub. This is done for a few reasons, including higher efficiency while operating in reverse gear, not to mention that propellers with simple geometry tend to be cheaper to procure or repair in the event of damage. Simplicity in this design aids several factors, from producing the hub and blade design to calculating the pressure distribution and analyzing the finite element model. Moreover, a less complex blade was easier to fabricate.

The finite element analysis portion of the project began with the simple analysis of the

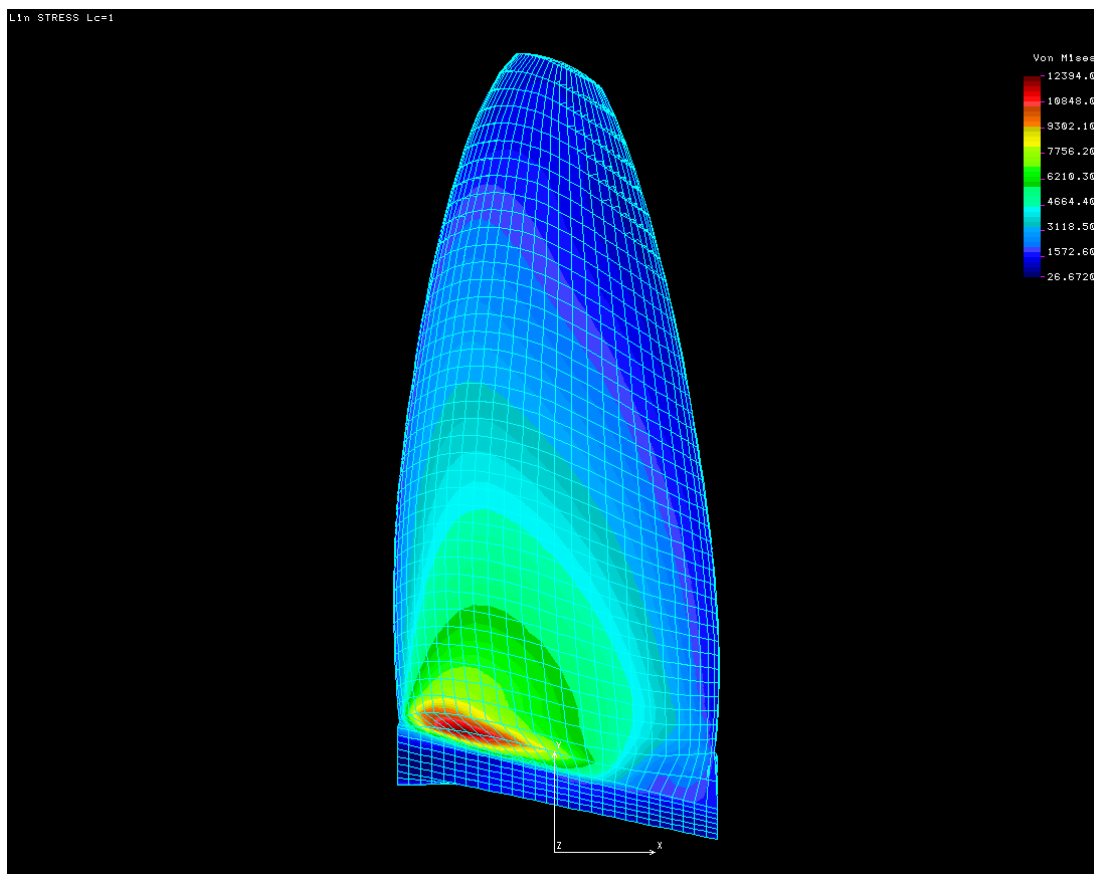
nickel-aluminum-bronze blade without the dovetail. The NAB blade provided a solid baseline for load case and element validation and confirmation. With points along the root section fixed in all-rotations and all-translations, the static pressure load was applied. The result of the finite element analysis showed the 12,000 psi design stress was evident near the root section. One should consider in basic terms how a propeller blade acts under a particular load condition. Take, for instance, a flagpole cemented into the ground. When the wind blows, it acts upon the flagpole and causes it to bend. The area of highest stress is in the section of the flagpole closest to the ground, as the bending moment is greatest at that point. The force on the pole created by the wind multiplied by the distance to the base of the pole equals the bending moment due to the wind. Based on the geometry and material properties of the flagpole, the peak stress can be calculated. The wind force acts at a point on the pole known as the center of pressure. Air and water are both fluids and differ primarily in their density and their other corresponding kinematic factors. The most important thing to take away, perhaps, is the idea of center of pressure. In the flagpole scenario, the force and center of pressure were produced based on the drag of the pole in the breeze. Say the wind is blowing from right to left and the flagpole is cylindrical. The lift force generated by the fluid (air) passing over the flagpole would be directed both into and out of the page. Because the flagpole is cylindrical, those lift forces are equal and opposite in direction; therefore, canceling each other out. The drag force, however, remains in the direction parallel to the airflow, pointing toward where the wind is going. This force causes the flagpole to deflect.

A similar, slightly more complex situation occurs with a marine propeller. As the propeller turns, the fluid (water) passes over the blade surface. Instead of being cylindrical in nature like the flagpole, each blade section is designed to produce some amount of lift due to its shape. Bernoulli's Principle and circulation theory explain that when a fluid passes over an

object, lift is produced due to a pressure differential induced by a corresponding velocity differential. This lift force occurs perpendicular to the flow line, while a drag force acts in a parallel direction. Other than the difference in fluid, a major difference in the mechanics standpoint between the flagpole and the propeller is the dominant force. The propeller's structural design is driven by the amount of lift (thrust) produced by the blades' motion through the fluid. The drag force is much less significant.

As the wind force acts through the flagpole's center of pressure, so do the propeller's resultant forces. A simple finite element analysis of a propeller blade models the thrust force as a point load through the blade's center of pressure. While simplistic, this method works to

Figure 11 – Bronze Stress Plot



quickly check the peak stress without requiring the interpretation of the complex pressure distribution. However, the point load approach gives incorrect stress results around the center of pressure and radially outward to the tip. No force is applied to those elements using this method, whereas in reality, pressures are distributed over the entire blade. Despite its more limited applicability, the point load method was used to confirm the more complex computational fluid dynamics calculations, as well as the geometry and boundary conditions of the finite element model.

The advent of computational fluid dynamics, in this case lifting surface and panel codes, has allowed for the potential decrease in material factors of safety for propellers and more accurate structural analysis, especially when combined with modern finite element methods, leading toward lighter and lower cost propellers. This particular model for the Yard Patrol craft yields results very similar to what the original design case was likely to be. The peak stresses occur near the root with a magnitude of close to 12,000 psi and a maximum tip deflection of approximately one tenth of an inch over a twenty-two inch span. Figure 11 demonstrates the NAB von Mises combined stresses for the dovetail blade. Bear in mind that this was the faired propeller geometry where the hub fillet was essentially removed. Common thought is that the hub fillet is a structural component of the propeller when in fact it is not. Instead, it is used as a fairing method to improve flow over the blade near the root section. Even though the fluid velocity closer to the hub is significantly decreased, a faired shape would still improve efficiency by decreasing drag. Also, the factor of safety commonly used for a propeller blade without the hub fillet is approximately two. The added material in the root section not only improves water flow, but also boosts the factor of safety margin.

Encapsulated Propellers

This project also had an intermediate analysis step concerning the encapsulated propellers. While an encapsulated propeller does not relate directly to one built with composite materials, it does attempt to bridge the gap between traditional NAB propellers and the modern-day need for cheaper and more easily repaired ship propulsors. As explained earlier, the encapsulation method takes a cast NAB or stainless steel core and applies a layer of polyurethane on the surface. This coating was intended to resist impact damage as well as the effects of biofouling. What was unclear, however, was any sort of hydrodynamic disadvantage to using this method. The results from the encapsulated propellers' full-scale testing will be discussed later. Finite element analysis was not warranted until chief boatswain's mate Kenneth Mills, officer in charge of YP677, reported that his ship was pulling noticeably to the starboard side. Many possible causes could be eliminated since the problem did not exist before the

Figure 12 – Encapsulated Props on YP 677



encapsulated propellers were installed. This type of pull to starboard was due to a thrust differential between the two propellers where the port side was producing more thrust, either because it was more effective or the starboard side was less effective. Figure 12 shows both encapsulated propellers mounted on YP677.

An obvious difference between the two propellers was their core material. The port side propeller was cast stainless steel, specifically CA6NM, while the starboard side was NAB. This translates to significant difference in material stiffness, as the stainless steel has an elastic modulus nearly double that of NAB. Results from the finite element program reflected the difference in stiffness as the propeller tip deflection decreased from approximately one tenth of an inch for NAB to five thousandths of an inch for stainless steel. The difference in tip deflection would not cause a significant thrust differential. The focus shifted to the encapsulant coating as little manufacturing tolerance was imposed on its thickness. In some areas, the coating was approximately one eighth of an inch thick while in other regions it was almost twice that thickness. Overall, the blades are thicker than an unencapsulated propeller, which could lead to slightly higher thrust output at similar rates of rotation. Since both of these propellers were encapsulated equally, this possibility was ruled out.

If few tolerances were imposed on the actual thickness of the blade, perhaps a similar looseness would be present when the leading and trailing edges were formed. The edges are especially important since they affect the flow separation point. If the water flow begins to separate at a point before the trailing edge, it can effectively change the blade shape, increasing drag and reducing lift.

The CFD codes used at NSWCCD have several different options for trailing edge design, but none could account for this sort of temporary or inconsistent thrust reduction. Additionally,

there was no way to say whether this phenomenon was occurring on all three blades of the starboard propeller, or only one or two at different times. Over time, Chief Mills reported less pulling; possibly because he got used to it, the phenomenon naturally lessened, or there were unique weather conditions when it first occurred. Initially, the most probable explanation was temporary thrust reduction due to leading or trailing edge shape. The difference in tip deflection would not change the thrust characteristics of the propeller so drastically.

Composite Bladed Propeller

The most challenging finite element modeling came with the analysis of the composite blade. In the other models, the dovetail was omitted out of a necessity for both simplicity and a known baseline. By itself, the nickel-aluminum-bronze blade confirmed the load case before a significant change in geometry was made. Before the analysis could proceed, the dovetail geometry needed to be joined with the existing faired propeller plot. COSMOS/M required the structure to be built within the finite element program -- a complicated task when the desired geometry twists at various angles. Importing the geometry from the 3-D modeling program proved problematic, since the modeling program used too many spline curves to create the desired effect. The finite element program dealt better with points, lines, and uncomplicated planar surfaces.

Using corner point coordinates taken from the three dimensional model, corresponding points were established in the finite element model. Connecting these points to form a surface and transforming the set of surfaces into a volume provided a frame for element creation. The next step was to fill the gap between the bottom of the propeller geometry and the dovetail. The finite element model was produced with a slightly different method than the Rhinoceros-3D model as the geometry used in the finite element program was more of a geometric approximation. To create a small fillet, the bottom row of elements was first deleted from the blade model. A new row was then constructed, linking the dovetail and propeller geometries while avoiding the issue of element angles being too sharp for reliable analysis.

The small fillet, though not included in the 3-D model, would be fashioned by hand during the fabrication process. There were several trade-offs by creating the dovetail in this manner. Unlike the three dimensional model, the surface of the dovetail closest to the center of

the hub was not curved. The finite element model used a straight-line surface in that instance. Additionally, there were no corner fillets. These modifications, if anything, were conservative in nature. The fillets, for instance, were used to prevent the formation of stress concentration areas. The dovetail approximation lent itself more to stress concentration regions than the actual design, but the final results did not indicate a problem as the areas of high stress were located around the root section of the blade. Propeller loads were able to spread out over a larger area with decreased magnitude, but the stresses at the corners did not indicate that the geometry approximation had any significant drawback.

Once the full blade model was established, the next step was to determine the boundary conditions. The boundary condition determination seemed to be more complicated without being able to physically see or touch the blade and hub. Using the small acrylic model, one could see the contact points when pushing on the blade as if it were under load. The difficulty in modeling these boundary conditions is that they were nothing more than physical contact points as opposed to a mechanical restraint like a clamp, weld, or screw. There are specific methods for modeling these conditions, but some may generate inaccurate results without intricate model setup. The “visualization method” used for this project provided comparable results without added time investment.

The boundary conditions did not fix the blade in position with respect to the forward/aft direction, since the blade is only wedged in place. Additionally, there were as It is very difficult to fully and realistically constrain a given point about all three axes of rotation. Therefore, no points were rotational constrained. All of the other translation limitations were either in the y-direction, z-direction, or a combination of the two – depending on the point’s location in the structure. This was a form of an “elastic foundation” boundary condition, where the rotational or

translational constraints are tailored more toward a specific load condition.

The first stages of this analysis process, specifically the load verification on the unmodified NAB blade geometry, used a fixed boundary condition set where all of the points along the root section of the blade were unable to move (translate) or rotate in any direction. This tends to be the harshest of all boundary conditions, yielding the highest, most concentrated stresses under a given load when compared to other boundary condition options. In general, the results of a fixed boundary condition stress analysis are considered to be the most conservative. The results from this particular model reflected that generality; the peak stresses were greater under the fixed condition and lessened appreciably with the tailored constraints.

When a structure is constrained due to contact with another component, the boundary conditions are seldom easy to model. While the “visual” method is often acceptable, it may not always be the most accurate. It is within an acceptable margin, but other methods exist that will often yield a more exact solution. One of these methods is the 3D-Truss approach, where certain points are held in place by a three-dimensional truss element. A 3D-Truss element is similar to a piece of metal attached to an object along a given axis. This piece cannot rotate. Connecting one end to the structure and the other to a fixed point creates the boundary condition. Rigid body motion due to insufficient constraint occurred when this method was first attempted on the propeller blade model. Adding angular trusses solved the problem, but created a new issue: false stress concentrations. Since the dovetail was supported at the few truss connections, the structure would press more at those points than anywhere else. Smaller areas yield greater stresses if the force remains the same, per the definition of stress (force divided by area). Adding more trusses – thus creating a more realistic boundary condition profile – was a solution to this problem. However, the end result would likely have been very similar to the constraints

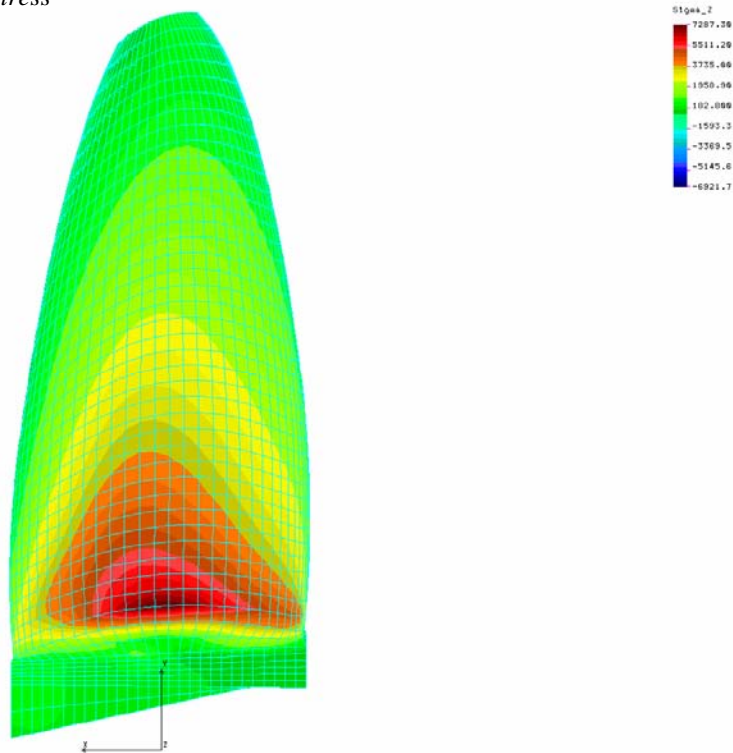
established by the visual approach.

Once the load case was confirmed, the dovetail geometry created, and the boundary conditions set, the stress analysis began. It first started with the NAB case, to see how the stress values were affected by the modified geometry and the location of the highest concentrations. The values decreased to some degree, likely due to the boundary conditions, as well as the additional material present around the root section and foundation of the propeller blade. Then, the element type changed from “Solid” to “SolidL,” or solid laminate. The user is able to input the number of layers within the laminate, the material for each layer, and the angle of the fibers with regard to the reference axis which was an imaginary line running from the center of the dovetail to the tip of the blade. Five ply groups of carbon cloth: forty percent of the fibers oriented parallel to the reference axis, forty percent perpendicular to the reference axis, and twenty percent at +/- forty-five degrees to the reference axis were chosen to comprise the fiber layout.

This laminate architecture is similar to that of a beam under a distributed load – an approximation used in the early stages of propeller design to determine initial strength requirements. Each element was assigned this material ratio instead of specifying actual ply group thicknesses. This method streamlined the analysis without significant loss of accuracy. The forty-five degree cloth was intended to be the shear-bearing material. Despite the largest shear being present at what would be considered the propeller’s neutral axis (the imaginary line through the centroid of the structure), the forty-five degree cloth was inserted every fifth ply, creating the specified twenty percent content. The placement of this cloth prevented the formation of shear hotspots, effectively spreading the shear strength over the entire laminate instead confining it to one specific section.

LIN STRESS Lc=1

Figure 13 – Through the Thickness Stress



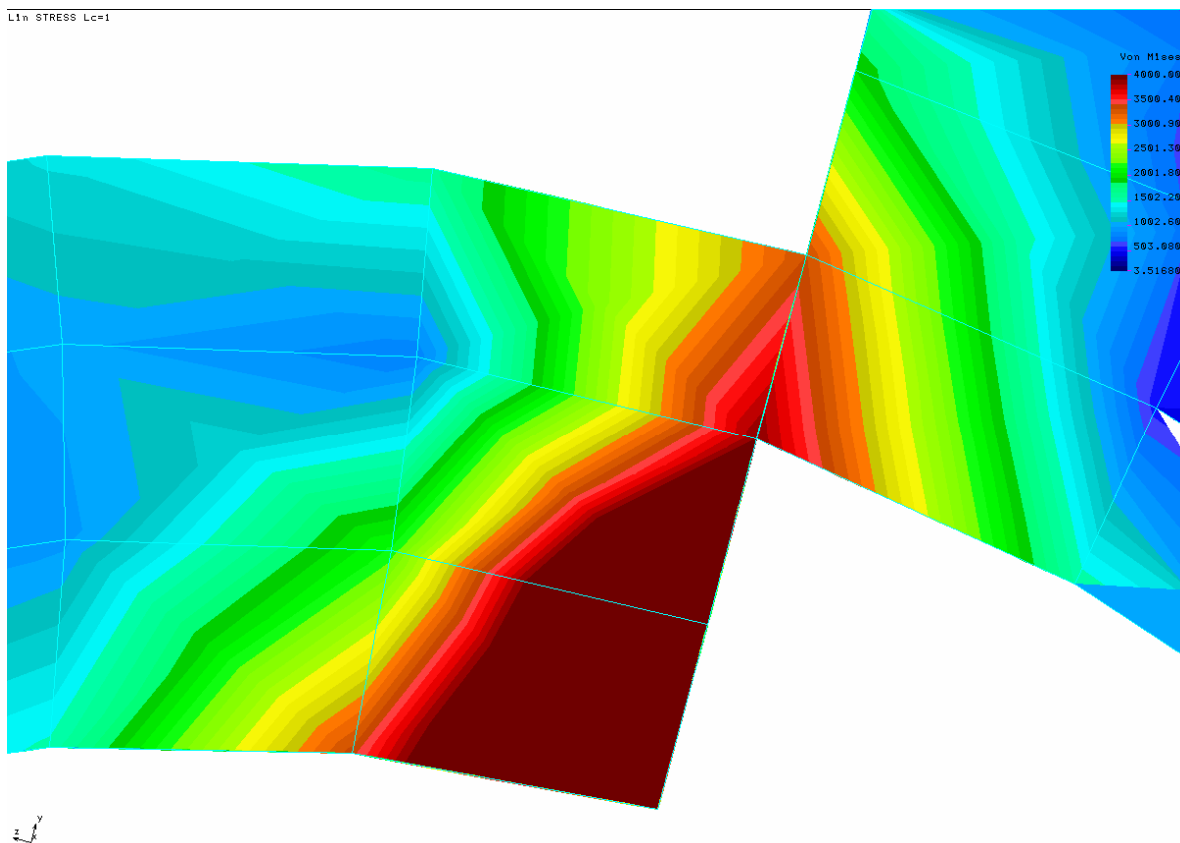
Loading the laminate propeller yielded some interesting results. The maximum tip deflection increased to approximately 0.2 inches, as opposed to the 0.1 inches seen with the NAB propeller. Given the carbon fiber laminate was two-thirds as stiff as the NAB, the deflection values seemed reasonable. Unlike isotropic materials where the stresses may be combined as the von Mises stress, stress combination can be inappropriate for composite structural design. One of the best approaches is to analyze the stresses in each direction, for each ply of the laminate. Doing so for this propeller blade yielded two important conclusions: the amount of carbon fiber used was an ample amount, as no factor of safety (FOS) for the fiber was below the equivalent FOS for NAB, even with a twenty percent uncertainty margin added for fabrication; and, the weakest point was the resin portion of the composite matrix. Figure 13 shows the nearly unsatisfactory levels of σ_z – the maximum compressive or tensile stress “through the thickness” of the blade and the corresponding high stress areas. Appendix C shows a more detailed factor

of safety breakdown. These factors of safety may be somewhat misleading if the propeller's tip displacement was too great. The effect of bending stress was apparent; the greater the bend, the greater the stress along the outside edges. Adding uni-directional fiber to decrease the total tip deflection would relieve this problem, as well as allowing the epoxy to cure at a higher temperature to increase the laminate strength. The primary conclusion is if the blade fails, it would be due to epoxy yield, not due to the lack of fiber strength.

NAB Hub

The last leg of the finite element analysis was to ascertain the strength of the dovetail cut through the hub. Figure 14 shows the area of greatest combined stress in the NAB hub. Creating this sort of geometry, even utilizing the approximation method in creating the propeller dovetail, would be a cumbersome task given the lack of interaction between the three dimensional and finite element modeling programs. Instead, the hub was modeled as a hypothetical worst case; where the edge of the dovetail cut would be on the same radius as the edge of the keyway,

Figure 14 – Stress Riser at Keyway/Dovetail



creating a potentially dangerous shear concentration. Using the reaction forces from the blade analysis as the load condition, as well as a more fixed, visually determined set of boundary

conditions, the model was analyzed. Doing so yielded stresses less than 4,000 psi – well within the safety margin for nickel-aluminum-bronze, which has a yield strength of (up to) 75,000 psi. Even so, this model was conservative. No fillets were modeled and the radial distance between the inside of the dovetail and the outside of the keyway was smaller than the actual design, because element size prevented exact placement. Moreover, the hub was created to avoid this worst case scenario: the keyway was placed in such a manner as to avoid the edge lineup. The actual hub has significantly more shear area, further decreasing the shear stress.

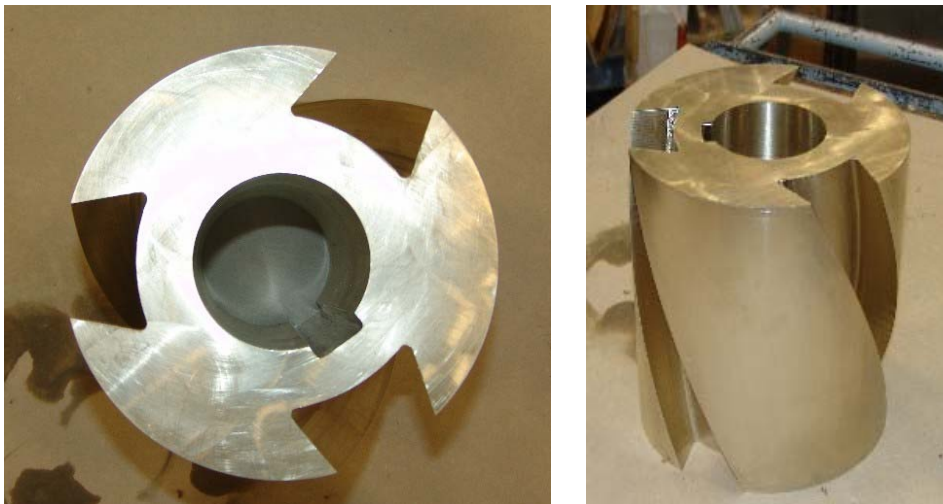
Fabrication

NAB Hub

Upon completion of the analysis portion of the project, the next step was to make the theoretical designs a reality. Possibly the most difficult portion, since it relied heavily on outside personnel, was the hub fabrication. Mr. Edward Gerding and his team at Boeing Phantom Works in St. Louis, Missouri developed a timely solution. The original intention was to use SLS fabrication. SLS, or selective laser sintering, is a method of rapid prototyping which uses a metal dust melted by a laser, as it creates the structure one layer at a time. Conveniently, the Boeing SLS machine is capable of using a nickel-aluminum-bronze dust; however, the "print head" used to create the part was too small to create a full-scale hub. The use of the SLS technology would have been mutually beneficial, as Boeing would be able to test a full-scale load-bearing part while a hub could be rapidly produced with a complicated dovetail cut without the machining expense.

Instead, the machine shop at the Boeing plant would attempt to manufacture the part so long as the material and the design were provided. At first, the design was sent to their computer aided machining technicians for their perusal. Their response was that it would take as little as a

Figures 15 & 16 – NAB Hub



day and a half to program the cutting routine and an additional day to machine the piece.

While waiting for the nickel-aluminum-bronze cylinder to arrive, a test piece from aluminum was cut. What may have taken months to produce elsewhere was manufactured and shipped by Boeing in just over a week. The bronze hub is shown in Figures 15 and 16. The remainder of the fabrication work remained in the hands of Naval Academy personnel involved in the project.

Composite Blades

The fabrication of the blades was a multi-step process beginning with the fiberglass mold. From the three dimensional computer model of the blade and dovetail, Mr. Paco Rodriguez at Naval Surface Warfare Center -- Carderock Division used his SLA machine to create one of the largest prototypes he ever made: a twenty-two inch epoxy propeller blade model to be used as a mold plug. The first step in the mold fabrication was to create a parting line; a line located approximately half way between the two sides of the blade located along the edges where the mold would separate. Figure 17 shows the plug prepared for fabrication. Using a thin strip of Masonite and Bondo as a tack welding compound, a flange was set along this parting line. Sharpening the edge with the corner of a razor blade was crucial to creating a definitive mold. Once the surface was free of excess Bondo and other gouges, mold release compound was applied to keep the gel coat and epoxy from bonding to the plug.

These were to be temporary molds, with minimal cost and thermal stability requirements in mind. Ideally, they would have been produced in almost exactly the same manner as the blades to fabricate a more permanent mold. Using the same material and epoxy, as well as similar fiber alignment, would create a thermally stable mold which would not deform or warp if treated correctly. The fiberglass prevented elevated temperature post-curing of the carbon blades for fear of permanent deformation.

Figure 17 – Plug with Flange



For an effective mold, a smooth surface is absolutely necessary, especially if complex geometry threatens to lock the plug and mold together. The last thing one needs to worry about is whether the surface is too rough for proper release. Additionally, any roughness in the mold surface translates to the final blade, requiring a more intense finishing process. Fiberglass gel



Figure 18 – Mold Fabrication Setup

coat, similar to that used on many pleasure boats, provided this smooth surface when applied correctly. Once the gel coat was spread evenly over the surface (slightly thicker over the complex geometry of the dovetail) and began to thicken to the point of tackiness, a pliable layer of fiberglass was laid down.

From this point forward, it was a matter of applying more layers of fiberglass for reinforcement. Supporting layers were a mix of very heavy boat-weight cloth and a somewhat lighter woven roving fabric. The epoxy used to bind the structure together was the same as that used in the blades: West System's Pro-Set 125 resin with the accompanying 229 hardener. After the laminate cured, the sharp glass edges were ground off and the opposite side of the plug was prepared for the same process. The Masonite was removed to expose the composite flange and allow a tight fit between the two halves of the mold. The final steps, after both sides were cured, were to remove the plug, reapply mold release to both sides, and build makeshift foam legs to

Figure 19 – Cutting Area



create a stage for the blade lay-up process.

Figure 18 shows the initial mold fabrication setup.

The general philosophy of becoming independent of the molds as quickly as possible guided the blade fabrication process.

Due to the complex geometry of the dovetail

area, continuing to lay material into the mold could have caused problems as the plies accumulated. As a sacrificial layer, one ply of fiberglass was used as the outermost layer. It was then followed by three layers of carbon fiber to create an impermeable shell. Several more plies of carbon fiber were laminated to ensure geometric stability before the piece was “independent” of the mold. Every fifth ply of carbon fiber had a bias of plus and minus forty-five degrees from the reference axis to satisfy the twenty percent requirement established because of shear stress concerns.

The laminate schedule, or order in which the plies were laminated, was determined on a day-to-day basis but conformed to the global laminate objective. Layers were cut using a

Figure 20 – Ply Stacks



“quilting wheel” (Figure 19) and stacked into piles for lamination the following day (Figure 20). Figure 21 shows the typical laminating setup. Since the plug was approximately an inch and three quarters thick at the widest point, it took weeks to

properly cut the plies and add them to the laminate at a pace of approximately 0.25 inches per day. Note that all three blades (six halves) were manufactured concurrently. At approximately 0.017 inches per ply, one quarter of an inch for three blades equaled forty-five plies per day. Cutting the shapes was no easy task, since ideally each ply would be somewhat smaller than the one preceding it. Once the epoxy had cured, the rough edges were reground the next day to more clearly define the shape and decrease the amount of sharp carbon ends exposed along the edges.

After the cut-laminate-grind cycle had been repeated enough times to accumulate ample thickness at the root section, the next stage was set to begin. Fitting the two halves of the blade together was a greater challenge than expected, with a significant amount of the carbon needing to be ground away for a proper fit. The end result, after many hours of leveling the high spots with an angle grinder, was three blades that were slightly thicker than the original plug, but fit nicely together.

Assembling the full blade required that the space remaining in the center be filled with a

Figure 21 - Laminating

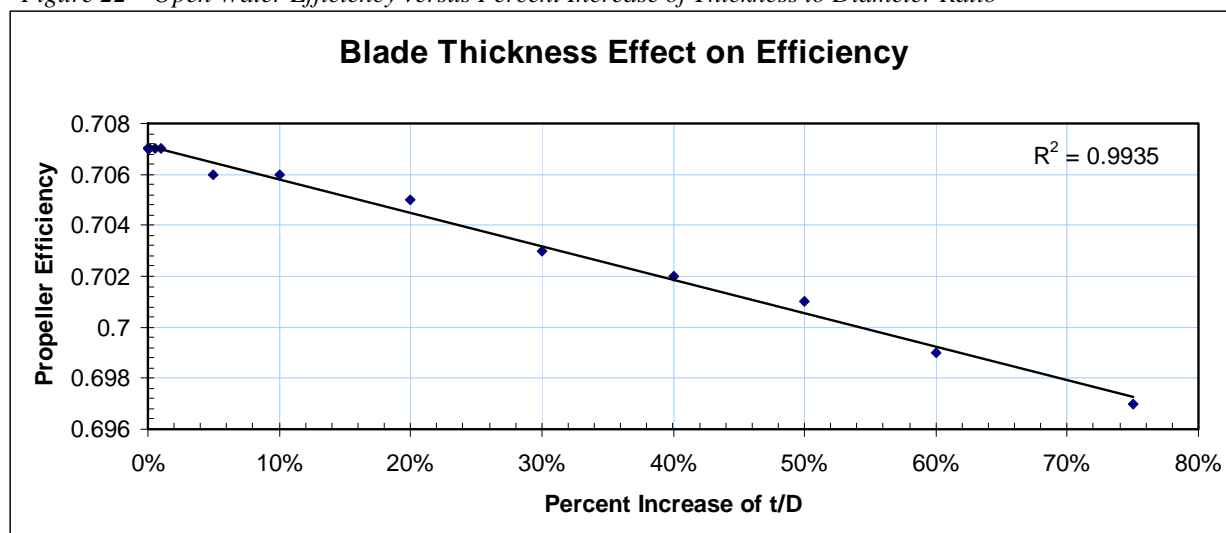


tougher and faster curing resin compound -- West Systems 105 resin with the corresponding slow hardener mixed with Cabosil and carbon dust. Any space remaining between the edges of the blade was eliminated using

the same epoxy-fiber dust compound while carbon tape was applied to smooth the edges and provide a shear transfer across the parting line joint. The final step before potting the blades in the hub was to round the edges and recoat the blade with a final layer of epoxy to fill any remaining voids on the surface.

There are some areas of concern regarding this particular method of fabrication. First of all, the blade is a slightly thicker overall than the original plug. This affects the lift characteristics of the old design. The increased thickness is not necessarily detrimental. In fact, more lift is generated over the thicker foil, provided that it has not become too thick to be

Figure 22 – Open Water Efficiency versus Percent Increase of Thickness to Diameter Ratio



effective. Up to a point, increased thickness can be a good thing with minimal loss to efficiency.

Figure 22 shows the effect on the efficiency if only the thickness to diameter ratio is changed.

The effect of the increased thickness will be qualitatively determined through full-scale testing.

Another potential problem is the creation of a void when the two halves were joined. A void in the center of a laminate can cause delamination and cracking, even if it is small and filled with a toughened epoxy compound. As the resin is usually the weakest part of the composite

laminate; a resin-rich area can sometimes lead to material failure. Finally, the balance of the blades due to the variation in grinding patterns and laminate architecture could cause increased vibration. It was unlikely that this would be as important an issue as it would be for a nickel-aluminum-bronze propeller, due to the significant disparity in mass between bronze and a fiber reinforced composite. Small variations in the weight distribution will not have near the effect as similar abnormalities in a bronze propeller.

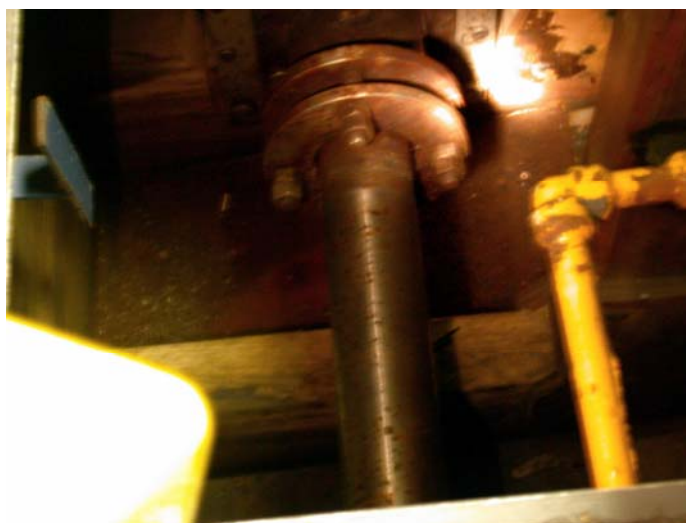
Full Scale Testing

Bronze and Encapsulated Propellers

A unique portion of this project was the full-scale testing of the Yard Patrol craft in an effort to gain some perspective on its current propulsive performance. The first phase, with the nickel-aluminum-bronze propellers, was to create a baseline for comparison. Subsequent tests would evaluate both the encapsulated and composite bladed versions. Enclosed in Appendix D is the original test plan designed for this phase of the project. Some pieces were shortened or otherwise modified due to resource constraints at Naval Station Annapolis. It is important, however, to see the intent of the original testing regimen for possible future testing.

Before testing could begin, the instruments required installation and setup. Without the help of Mr. Kenneth Remmers, Mr. William David Burroughs, Mr. Martin Donnelly (NSWCCD), and Mr. Gary Gibson (USNA), none of this would have been possible. Using their combined experience in full-scale experimentation, a comprehensive sensor suite was designed

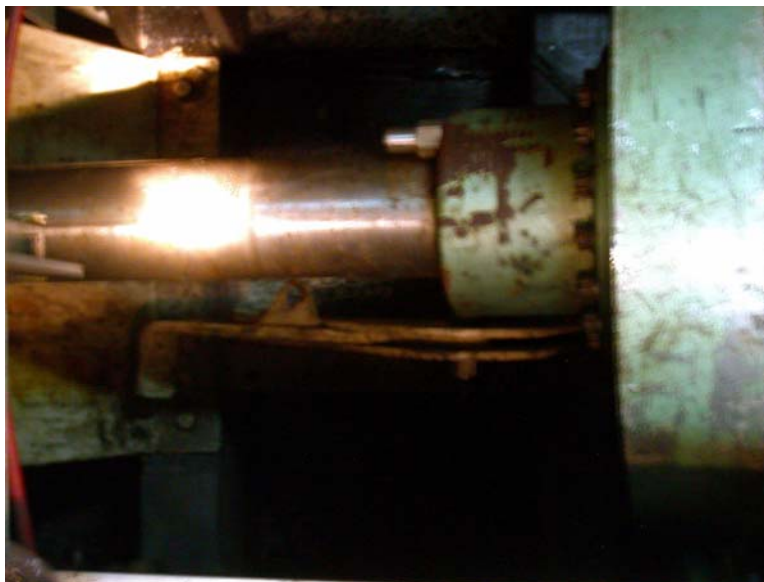
Figure 23 – Shaft Access



and implemented to gather information on each shaft's torque and revolutions per minute (RPM), as well as streamed global positioning output for speed over ground data. Mr. Gibson wrote the data collection code which took one hundred samples per second from the shaft strain gages to yield nearly instantaneous torque values and approximately one sample every three to five seconds for RPM. Speed data was a constant stream of location, time, and speed over ground information.

The bilge space between the thrust bearing and packing gland (where the shaft exits the hull) is cramped and vertical access is nearly impossible. Figure 23 shows this bilge space; bear in mind that the shaft in the center of the photograph was four inches across. Yet, Mr. Burroughs squeezed between the engine room deck stiffeners to complete the intricate task of aligning and mounted the torque strain gages on the shaft. For a few hours at a time, barely able to reach his

Figure 24 – Flex Coupling



own tools, he meticulously installed the torque measurement system. Calibration was not completed since the ship was in the water. The RPM infrared sensor had to be mounted in the plane of the reflective loop and approximately one foot away from the flex coupling. The wide,

green strip framing Figure 24 is the flex coupling (joint that connects the engine to propeller shaft), where the reflector strip was mounted. The infrared sensor worked by the principle of a “true or false” type system. If the broadcast signal hit a reflective strip located on the flex coupling, a direct current pulse of ten volts returned to the data collection unit where the pulse was counted and averaged over the time period, yielding RPM. The location for this sensor was in a minimal access area just aft of the engine.

The most difficult information to collect and sort was the GPS data. The receiver transmitted the data to the collection unit, but somewhere along the line data was stored in a buffer; the effect was that time sensitive tests like acceleration or emergency stop would be filled with old data. Establishing a new collection code and a computer system assigned solely to its collection resolved the issue and further increased the sample rate of the other sensors.

There were several reasons for full-scale testing of the Yard Patrol craft, as opposed to using a towing tank or water channel. When the testing was scheduled to begin, the USNA Hydrodynamics Laboratory’s 380-foot towing tank was out of commission due to Hurricane Isabel the previous year. The model propeller testing apparatus was too large to operate in the 120-foot tank. Isabel’s damage to the circulating water channel was repaired in time for a possible cavitation study, but time and resources were insufficient. Additionally, there was an appreciable difference between the pitch versus diameter distributions of the model and full-scale Yard Patrol propellers. While this discrepancy could have been repaired by adjusting the flow rate and revolutions per minute within the circulating water channel, the reality was that the propellers were physically different and should not be considered direct models of one another. Without this direct correlation, time was better spent working on the full scale model as opposed to machining, manufacturing, and testing a smaller version.

The overriding reason for testing on the full-scale vessel was the lack of scale factor. Scaling ship models or other structures can be reasonably straightforward, but a general rule of "bigger is better" applies when experimenting with hydrodynamics. Few things scale directly, specifically objects that interact with the fluid system and for that reason, testing a full-scale propeller is often more beneficial than a model, depending on the possible flow regimes the blades may experience.

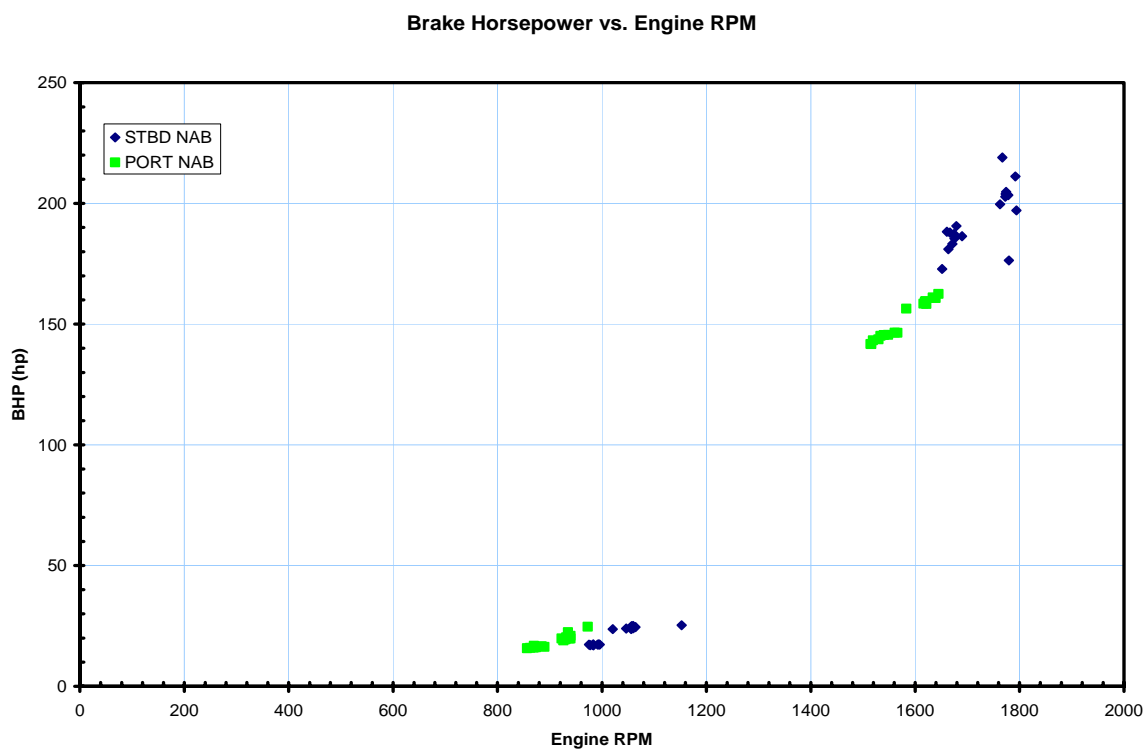
A deepwater full-scale ship test requires certain criteria must be met. If the depth is too shallow underneath the keel, the ship may experience what is known as blockage -- an augmentation of the ship's resistance due to the flow interaction between the hull and the ocean floor. A similar situation can occur in a towing tank if the model vessel has too wide a beam or too deep a draft. Calculations for the YP drove the required depth to at least eighty feet to prevent blockage. The area surrounding the U.S. Naval Academy, both in the Chesapeake Bay and Severn River, is reasonably shallow -- far less than the required depth. An area approximately one nautical mile long with a mean lower low water sounding of no less than eighty-five feet was located on the eastern edge of the Bay Bridge shipping channel.

The first run of nickel-aluminum-bronze propeller tests was made 14 November 2004. That day was the first time an attempt at data collection on a full-scale ship trial was made using the instrumentation setup provided by NSWCCD. With the first experiment came many programming glitches and data inconsistencies. Weather conditions were light winds and waves less than two feet. This would be one of the last acceptable testing days, due to the weather and scheduling requirements until the following spring. Much of this day was lost modifying the GPS collection program to gather current data as opposed to information stored in an obscure buffer memory. Adjustments were made allowing testing to proceed in the afternoon.

Results from this test period seemed questionable, as the power curve versus Froude number (a nondimensional ratio relating speed and length in a given water density) has an unusual hump at approximately seven knots. This grouping of data was significantly higher than the power required at twelve knots. The plot in Figure 25, however, shows a powering curve consistent with what would be expected. Unfortunately, no data points represent the span between 1100 and 1500 RPM. The error seen in the results is likely due to inexperience with full-scale testing, the lack of multiple days of tests, as well as possibly mismatched GPS data. While only some of the data collected on test day appeared unusual, further analysis indicated the results seemed to require confirmation. However, YP677 had already been hauled from the water and had her NAB propellers replaced by their encapsulated counterparts.

The testing of the encapsulated propellers went much smoother than the first NAB runs. The test plan was changed to collect the most pertinent data: straight line runs at various speeds. Ideally, the data pertaining to speed and torque could be nondimensionalized to yield torque

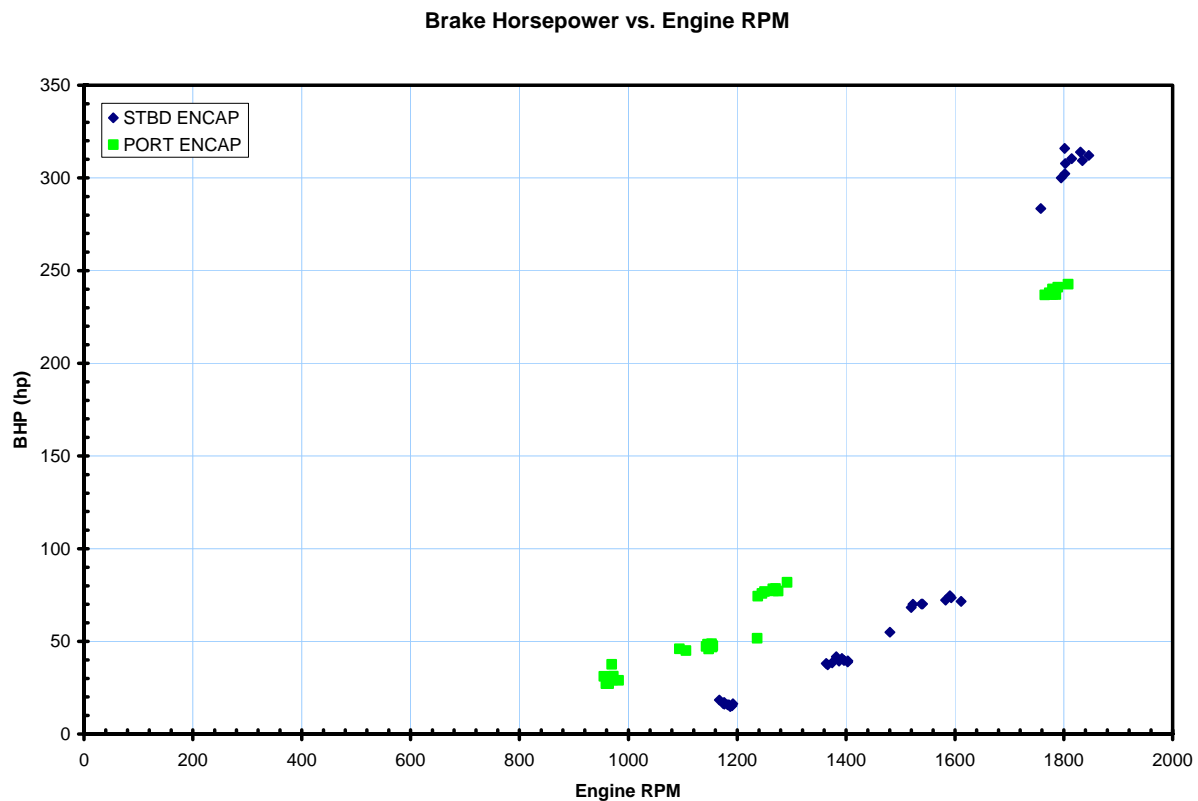
Figure 25 – Brake Horsepower versus Engine RPM for Baseline Test



characteristics of the propeller. To effectively generate this curve, however, data over a wide range of advance coefficients (J) is required. Full scale testing reveals an important problem: a propeller can only experience a small range of advance coefficients in full-scale operation. This is a particular instance where towing tank or water channel testing is very valuable, since flow rate is uninterrupted and may be adjusted for a wide range of speeds making it possible to plot nondimensional curves over a much broader spectrum of advance coefficients.

Testing this particular day in December was accomplished in harsh weather conditions, with high winds and waves greater than four feet high. The data collected in the form of a ship's power curve appeared fairer than the original nickel-aluminum-bronze runs. Figure 26 shows the data points collected. Note the disparity between the port and starboard encapsulated propellers. However, there is room to doubt these results since waves significantly affect the resistance of

Figure 26 – Brake Horsepower versus Engine RPM for NAB Test



the ship in a nonlinear manner, making adjustments inaccurate.

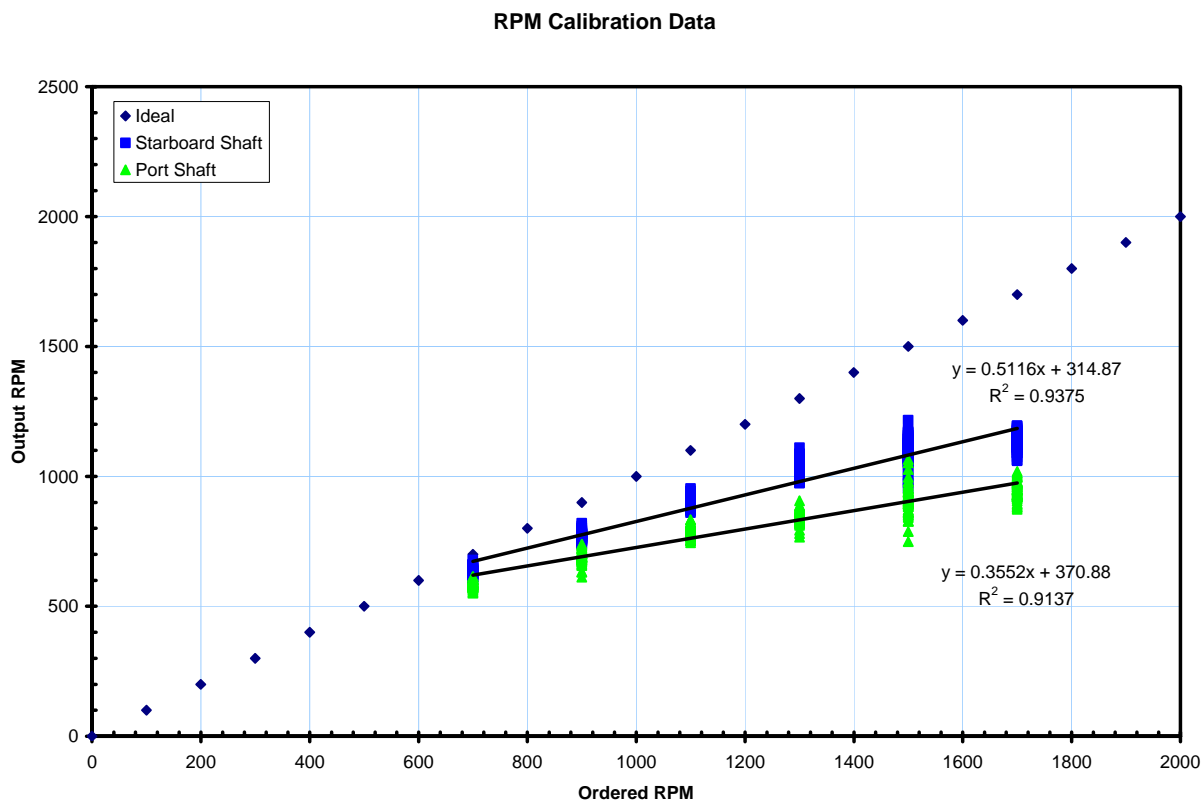
After the data analysis occurred and the common inconsistencies were noted, it seemed worthwhile to begin searching for errors in the instrumentation stream. At first it appeared the most ambiguity would stem from the strain gages implemented to read each shaft's torque. The gages were applied in confined quarters, so alignment could have been adversely affected. Additionally, the gages selected were chosen for their increased accuracy despite their shorter life expectancy. Over time, their quality would degrade more quickly than similar gages. The difficulty eliminating the possible error was the lack of calibration. The shafts were never calibrated due to accessibility issues. Furthermore, the system had a past history of negligible error without the need for dry loading the propeller. These factors led to the decision to use torque calibration as a last resort and to continue operating under the assumption the gages were accurate to within five percent. The gages were installed by an experienced technician and both shafts output similar values for the torque required to rotate the shaft by hand from rest. Perhaps a more significant error source could be found elsewhere, namely the RPM collection system.

There were several considerable variables concerning the RPM pickup arrangement and collection mechanism. As explained earlier, when the sensor receives the reflected beam it sends a pulse voltage back to the "totalizer," which records the number of pulses per time step. If the sensor is too close or too far away, or is canted at an incorrect angle, pulses may be merged or dropped. A way to determine whether the pulse stream was normal was to feed the output into an oscilloscope to visually inspect the waveform. With some data acquisition units, it is possible to record these pulses for more in-depth analysis – a feature that would have been helpful in this case. Basic visual analysis indicated that few pulses were dropped or merged. At higher speeds, a few seemed to merge together, but still approximately ten percent or less. Seeing nothing

visually out of place, it seemed appropriate to design a small experiment that would compare an engine order to the engine result. For instance, if the ship operator calls for 800 RPM and the pick-up reports something different, an error would be apparent.

The results of this test (Figure 27) indicate a clear disparity in the actual RPM versus the ordered RPM. While there is some scatter in the data points at each RPM (specifically the higher orders), it may be due to the number of significant figures reported in the time step. Each time

Figure 27 – RPM Calibration Results (Encapsulated Propellers)



was expressed to the nearest one-hundredth of a second. At high rates of revolution, more significant figures in the time data would have been helpful. More important than the scatter, however, was the visible trend difference between the ideal and observed RPM curves. For some reason, neither of the engine revolution rates was as high as one might expect. Thinking this was the source of the problem; an effort was launched to square these gages away. Figure

27 demonstrates the RPM calibration curve results.

A final step was to re-inspect the data analysis code (Appendix E) written to deal with the raw numbers in an effective manner. A typical Excel workbook for one of these tests had upwards of fifteen worksheets, each with about 4500 rows of strain information. Nothing in the code seemed to lead to this sort of error. The code itself had significant user control and was capable of dealing with these large files.

On 19 April 2005, the encapsulated propellers were removed from YP677 in the process of overhauling the port engine, giving the first glimpse of the effects of several months of use on the vessel. The only significant sign of wear was one blade on the starboard propeller was stripped almost completely of its encapsulated coating. All of the other blades had maintained their original condition. With this revelation came several possible explanations for the data and performance notes taken since the mounting. The basis is that a propeller will produce more thrust at a given RPM if it has a marginally greater thickness. Some efficiency is lost as drag increases, but the drag increase is minor for small changes in thickness. This could be an explanation for why the vessel would pull to starboard, as Chief Mills had indicated. The starboard propeller had one blade that could not produce the same amount of thrust as its counterparts, so the starboard side propeller was effectively less powerful than that of the port side. This thrust differential caused the boat to twist to starboard.

Additionally, the loss of encapsulation would shift the power curve location (up or down) since greater power output would occur at a similar or lower RPM. Finally, it could explain the differences in the RPM calibration curve. The ship's gages were calibrated for NAB propellers, relating RPM to the required thrust for a given speed. If the thrust characteristic changes, the RPM gages in the pilothouse lose their accuracy. Since the RPM calibration took place with the

encapsulated propellers installed, the “standard line” can be eliminated from the calibration plot and the RPM order versus RPM output can be compared from one shaft to the other. Doing so shows that as RPM increases, the difference between the port engine and starboard engine outputs also widens. As the operator opens the throttle, more diesel fuel is injected into the cylinders, thus increasing power output. But the engine is only capable of a certain amount of power output, so at a specific setting (assuming the throttles were set the same), the port engine was able to turn the shaft less often (lower RPM) because the added blade thickness required more power. Of course, other explanations could be a difference in throttle setting or simply the difference in engine quality. The blade damage and resulting thickness distribution changes indicate the contrary.

Composite Bladed Propeller

On Wednesday, 27 April 2005, the U.S. Navy's first composite bladed propeller was mounted on YP696. In little more than two hours, she was hauled from the water, her original port side NAB was removed, the new composite bladed propeller was mounted (by two people without forklift assistance), and she was launched for sea trials. Figure 28 shows the composite bladed propeller being installed on the port shaft and Figure 30 shows

Figure 28 – Composite Propeller Installation



the final, installed propeller. Since a valve on the port engine of YP677 had been burned, YP696 was chosen as a replacement with one caveat: she could support only qualitative testing. As she

Figure 29 – Composite Propeller Test Results

Run	Engine	Engine RPM	SOG (kts)
1	STBD	850	4.7
1	STBD	1200	6.2
2	STBD	850	4.2
2	STBD	1200	5.7
3	STBD	850	4.2
3	STBD	1200	6.1
1	PORT	850	4
1	PORT	1200	5.9
2	PORT	850	3.8
2	PORT	1200	5.9
3	PORT	850	4.7
3	PORT	1200	6.4

PORT Averages	
850 RPM	4.17
1200 RPM	6.07

STBD Averages	
850 RPM	4.37
1200 RPM	6.00

% Difference	
850 RPM	4.58
1200 RPM	1.10

was backed from the Travelift slip, both engines were put aback at a two-thirds bell. The intent was to gingerly increase the RPM on the experimental propeller, but the exit from the slip pushed the envelope. In those first few seconds, the success of the propeller test was in the balance.

The vessel proceeded out of the NAVSTA Annapolis basin under power from both propellers. Once clear of any obstructions, the qualitative test procedure began. Remaining on the same heading to

allow maintain consistent current speed, each engine was isolated and run at 850, 1200, and later up 1800 engine rpm. The latter is considered the flank bell on a Yard Patrol craft. Figure 29 shows the results from these tests. The percent differences derived using the NAB as the standard show that the propellers perform nearly the same, within the range of allowable uncertainty. Additionally, 850 RPM is barely over the “clutch-in” speed for the Yard Patrol craft, so regulating the rotation rate was more difficult at the lower speed.

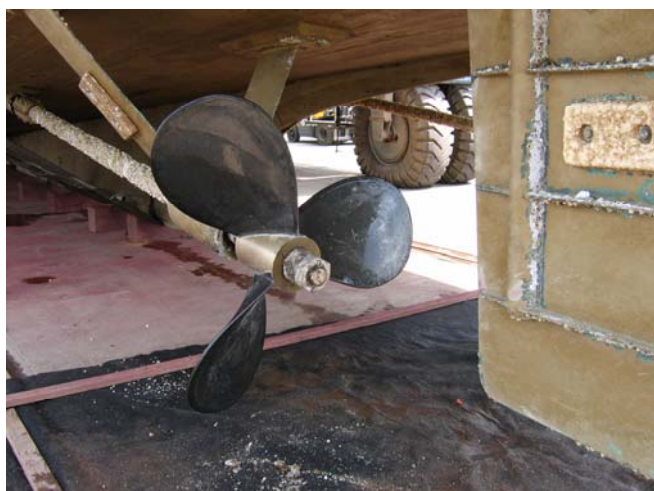


Figure 30 – Installed Composite Bladed Propeller

After about an hour and a half after launch, YP696 made the turn for the naval station. The port-mounted composite propeller was successfully tested at flank speed (~400 propeller RPM) producing a speed over ground of 9.1 knots. While this test was not repeated, it proved that the propeller could sustain the maximum

forward load available without failure. Testing was concluded with a half-hour run at flank speed (the wake is shown in Figure 31) back to NAVSTA Annapolis from the Bay Bridge shipping channel.

Figure 31 – Wake of Yard Patrol Craft at Flank Speed



Conclusions and Results

This project was groundbreaking work for U.S. naval propulsion, but it remains the tip of the iceberg. Undoubtedly, composite bladed technology holds great potential for the future of naval propulsion. Through the course of these studies several conclusions were drawn.

The use of rapid prototyping technology as well as three dimensional modeling and computer aided machining is an area of rapid growth and potential. At this time, if it can be conceived in the mind of an individual and modeled on a computer, the object can probably be made reality. SLA, specifically, played a crucial role in modeling the dovetail blade and hub, as well as the verification of the hub joint's fit. Without proper implementation of this technology, similar projects could be many times more costly in terms of monetary and time resources. With the potential for rather large parts to be manufactured almost autonomously once the "start" order is given, time is made available for other necessary research and preparation. An area that requires more study is the behavior of SLA (both the Invision3D acrylic and the NSWCCD epoxy mix) materials over time when exposed to moisture and heat. Initial claims made on the shape worthiness of the Invision3D acrylic seemed to be only partially true as it seemed to shrink by a small fraction in normal room conditions.

The full-scale tests on the YP could have been more successful if more time were devoted during the better weather portions of the year. Also, more testing over a period of several days would lessen the likelihood of a vessel or machinery casualty that becomes increasingly more likely to occur after months of use. A similar maintenance issue forced a premature end to the testing phase of this project. What was more important, though, was the testing of the encapsulated propellers and the feasibility of using an encapsulant on marine propulsors. What seemed like a good idea in theory resulted in a very good prototype. One

blade's loss of encapsulation should not spell the end for this technology, but rather serve as a solid starting point. Further study into polyurea/metal bonding methods could make this technology applicable on a wider scale. Additionally, continued study on the effects of cavitation on the encapsulant surface would be valuable to preventing similar damage on a composite bladed propeller.

Advancing the techniques of composite propeller fabrication could be one of the most significant contributions of this project. The fabrication process employed inspired several guidelines that would greatly increase consistency and decrease the cost of manufacturing composite blades. First of all, hand-cutting the carbon layers plies by hand can be time consuming and inconsistent. It is very difficult to decide the size of the smaller plies as they are laminated into the blade. Instead, larger plies were used and subsequently ground to size. The process of cutting the larger sheets, laminating them, and then grinding part of them away was very time intensive. A more consistent method would be to develop a topographical mapping program that could take a pitched blade and generate contour curves for each layer given the desired ply thickness. Sending these curves to a computerized numerically controlled (CNC) cutting table, each ply of a specific blade would be cut from the fabric rolled onto the table. Additionally, a carbon fabric pre-impregnated with epoxy ("pre-preg") would be easier to handle, as it does not deform when touched. Each ply of pre-preg carbon could be stacked according to reference lines and heated to the specified temperature, releasing the epoxy and binding the layers. Finally, it seems that a single part blade would be better than sandwiching two halves together. Such a process would be more applicable to a design with given reference lines and pre-preg fabric. The technology needed for successful development of this process exists in the United States at this time. Development of the topographical mapping code will be

the first step in streamlining the manufacturing process.

Avenues for further research are very broad, ranging from continued full-scale testing of the Yard Patrol craft, to model testing of composite bladed propellers, and follow-on cavitation studies of the smaller versions versus the bronze models. For research with a longer timeframes developing the topographical resolution code and corresponding machine path interpreter, determining a method of designing propellers to adjust to their load conditions by twisting or otherwise deflecting that is applicable to all types of propellers, and experimenting with various advanced composite manufacturing protocols are all worthy routes to follow. For a naval service that is constantly trying to advance its technological state, this iceberg seems like an exciting, unexplored wilderness with boundless potential.

Notes

¹ Bill Thomson, ed. “Carbon Fibre Propeller Saves Weight,” *Ship and Boat International*, (September/October 2003): 82.

² Jack A. Collins, *Failure of Materials in Mechanical Design* (New York: John Wiley and Sons, 1993), 426.

³ William F. Riley et al., *Mechanics of Materials* (New York: John Wiley and Sons, 1999), 351.

⁴ Niels Ottosen and Hans Petersson, *Introduction to the Finite Element Method* (New York: Prentice Hall, 1992), 1.

⁵ Edward V. Lewis, ed, *Principles of Naval Architecture* (Jersey City: Society of Naval Architects and Marine Engineers, 1988), II: 145.

⁶ Ibid, 145.

⁷ R. A. Higgins, *Properties of Engineering Materials* (New York: Industrial Press, 1994), 363.

⁸ Christos C. Chamis, “Probabilistic Composite Design,” in *Composite Materials: Testing & Design*, ed. S.J. Hooper (West Conshohocken: ASTM, 1997), 27.

⁹ Ibid, 39-40.

¹⁰ Ibid, 39.

¹¹ Ibid, 27.

¹² Ibid, 34.

¹³ Reifsnider, Kenneth L. “Durability & Damage Tolerance: Testing, Simulation, and Other Virtual Realities,” in *Composite Materials: Testing & Design*, ed. S.J. Hooper (West Conshohocken: ASTM, 1997), 50.

¹⁴ Ibid, 46.

¹⁵ Ibid, 49.

¹⁶ Nidal Alif, Leif A. Carlsson, and John W. Gillespie, Jr., “Mode I, Mode II, and Mixed Mode Interlaminar Fracture of Woven Fabric Carbon/Epoxy,” in *Composite Materials: Testing & Design*, ed. S.J. Hooper (West Conshohocken: ASTM, 1997), 101.

¹⁷ Ibid, 82.

¹⁸ M. Konig, R. Kruger, K. Kussmaul, et al. “Characterizing Static and Fatigue Interlaminar Fracture Behavior of a First Generation Graphite/Epoxy Composite,” in *Composite Materials: Testing & Design*, ed. S.J. Hooper (West Conshohocken: ASTM, 1997), 60-61.

¹⁹ Robert L. Sierakowski and Shive K. Chaturvedi, *Dynamic Loading and Characterization of Fiber-Reinforced Composites* (New York: John Wiley & Sons, 1997), 177.

²⁰ Ibid, 170.

²¹ Ibid, 173.

Works Cited

- Alif, Nidal, Leif A. Carlsson, and John W. Gillespie, Jr. "Mode I, Mode II, and Mixed Mode Interlaminar Fracture of Woven Fabric Carbon/Epoxy." In *Composite Materials: Testing & Design*, Vol. 13, ed. S.J. Hooper, 82-106. West Conshohocken: ASTM, 1997.
- Chamis, Christos C. "Probabilistic Composite Design." In *Composite Materials: Testing & Design*, Vol. 13, ed. S.J. Hooper, 23-42. West Conshohocken: ASTM, 1997.
- Collins, Jack A. *Failure of Materials in Mechanical Design*. 2nd ed. New York: John Wiley and Sons, 1993.
- Higgins, R. A. *Properties of Engineering Materials*. 2nd ed. New York: Industrial Press, 1994.
- Konig, M., R. Kruger, K. Kussmaul, et al. "Characterizing Static and Interlaminar Fracture Behavior of a First Generation Graphite/Epoxy Composite." In *Composite Materials: Testing & Design*, Vol. 13, ed. S.J. Hooper, 60-81. West Conshohocken: ASTM, 1997.
- Lewis, Edward V. ed. *Principles of Naval Architecture*. Vol. II. Jersey City: Society of Naval Architects and Marine Engineers, 1988.
- Ottosen, Niels and Hans Petersson. *Introduction to the Finite Element Method*. New York: Prentice Hall, 1992.
- Reifsnider, Kenneth L. "Durability & Damage Tolerance: Testing, Simulation, and Other Virtual Realities." In *Composite Materials: Testing & Design*, Vol. 13, ed. S.J. Hooper, 45-59. West Conshohocken: ASTM, 1997.
- Riley, William F., et al. *Mechanics of Materials*. 5th ed. New York: John Wiley and Sons, 1999.
- Sierakowski, Robert L. and Shive K. Chaturvedi. *Dynamic Loading and Characterization of Fiber Reinforced Composites*. New York: John Wiley & Sons, 1997.

Storch, Richard Lee, et al. *Ship Production*. 2d ed. Centreville: Cornell Maritime Press, 1995.

Thomson, Bill. ed. "Carbon Fibre Propeller Saves Weight." *Ship and Boat International*

(September/October 2003): 8.

Appendix A – Test Coupon Protocol

Introduction:

Fiber optic strain gauging methods are a new technology in the world of material load analysis. Such benefits include resistance to corrosion, better accuracy under certain circumstances, multiple strain gages on one fiber optic strand, and the ability to imbed the fibers. These benefits would be extremely useful in analyzing life cycle stresses on a particular structure. In the case of a composite propeller, utilization of such technology would be exceptionally valuable to understanding the loading and stresses involved in propeller operation.

Objectives:

1. Verify visual determination of diffraction grating location and orientation.
2. Determine loss of power due to bends in the optical fibers.
3. Validate optical strain gauging opposed to the voltage strain method.

Procedure:

Laminate Construction:

1. Prepare Mylar surface and work area.
2. Cut two four-inch by thirteen-inch strips of four-ounce glass fabric.
3. Cut four four-inch by thirteen-inch strips of Carbon-282 fabric.
4. Thread three optical fibers into a ply of Carbon-282 cloth. Be sure not to crimp the fibers too tightly. Each fiber will form a loop of a different radius, ranging from 0.5 to 1.5 inches, by 0.5 inch increments.

5. Thread the strand with the marked diffraction grating into the same ply, but parallel to the twelve-inch side. Thread an electrical strain gage as well, such that it's orientation measures strain in the same direction as the optical gage.
6. Place one strip of the glass fabric on the Mylar and spread the resin/hardener mixture evenly.
7. Repeat step six for the next four plies. Two plain Carbon-282 plies must be laid, then the threaded ply, and finally the second ply of glass cloth.
8. Cure as appropriate for the resin system.

Visual Inspection:

1. Visually note any areas of delamination, bubbles, and other flaws.
2. Visually note the location and orientation of the fibers, if possible.

Finite Element Analysis:

1. Create a finite element model of this test coupon.
2. In a cantilever beam condition, load the end with loads of five, ten, fifteen, twenty, and twenty-five pounds.
3. Tabulate the results, giving the stress at the same location as the strain gages.
4. Determine strain from the stresses calculated.

Laminate Testing:

1. Clamp the four-inch side as firmly as possible.
2. Load the end of the beam with individual weights of five pounds.

3. After each load is applied, measure the strains experienced by each of the gages.
4. Repeat steps two and three for weights of ten, fifteen, twenty, and twenty-five pounds.
5. Tabulate the results.

hide enter
pause
rotateface pause -7.25,0,0 7.25,0,0 120
pause
show
select pause
invert
hide
rotateface pause -7.25,0,0 7.25,0,0 -120
show
select pause
copytoclipboard
paste
pause
selnone
select pause
move pause pause pause
selnone
enter
enter
pause
selnone
select pause
scale 0,0,0 .99
selnone
booleandifference pause pause pause pause
pause
booleanintersection pause pause
selnone
booleanunion pause pause

Appendix C – Factor of Safety Information

Layer	Stress Direction	Material Properties	FEA Results	FOS	Acceptable?
1	σ_{xt}	85000	4454.00	19.08	19.08
1	σ_{xc}	65000	3477.70	18.69	18.69
1	σ_{yt}	83000	15195.00	5.46	5.46
1	σ_{yc}	55000	15505.00	3.55	3.55
1	σ_{zt}	13000	7287.30	1.78	1.78
1	σ_{zc}	17000	6921.70	2.46	2.46
1	τ_{xy}	19000	1229.20	15.46	15.46
1	τ_{yz}	19000	4316.40	4.40	4.40
1	τ_{xz}	19000	2914.20	6.52	6.52

Layer	Stress Direction	Material Properties	FEA Results	FOS	Acceptable?
2	σ_{xt}	85000	16314.00	5.21	5.21
2	σ_{xc}	65000	16057.00	4.05	4.05
2	σ_{yt}	83000	3694.60	22.47	22.47
2	σ_{yc}	55000	2901.80	18.95	18.95
2	σ_{zt}	13000	7161.50	1.82	1.82
2	σ_{zc}	17000	6993.60	2.43	2.43
2	τ_{xy}	19000	1291.30	14.71	14.71
2	τ_{yz}	19000	2981.60	6.37	6.37
2	τ_{xz}	19000	4268.60	4.45	4.45

NAB FOS	NAB + 20 %
2.11	2.31

Layer	Stress Direction	Material Properties	FEA Results	FOS	Acceptable?
3	σ_{xt}	85000	5317.20	15.99	15.99
3	σ_{xc}	65000	7098.20	9.16	9.16
3	σ_{yt}	83000	6238.70	13.30	13.30
3	σ_{yc}	55000	3270.10	16.82	16.82
3	σ_{zt}	13000	7040.50	1.85	1.85
3	σ_{zc}	17000	7073.20	2.40	2.40
3	τ_{xy}	19000	2304.60	8.24	8.24
3	τ_{yz}	19000	2787.20	6.82	6.82
3	τ_{xz}	19000	3233.80	5.88	5.88

Layer	Stress Direction	Material Properties	FEA Results	FOS	Acceptable?
4	σ_{xt}	85000	16573.00	5.13	5.13
4	σ_{xc}	65000	15008.00	4.33	4.33
4	σ_{yt}	83000	2816.80	29.47	29.47
4	σ_{yc}	55000	2392.50	22.99	22.99
4	σ_{zt}	13000	6907.60	1.88	1.88
4	σ_{zc}	17000	7129.20	2.38	2.38
4	τ_{xy}	19000	1347.80	14.10	14.10
4	τ_{yz}	19000	3085.30	6.16	6.16
4	τ_{xz}	19000	4149.00	4.58	4.58

Layer	Stress Direction	Material Properties	FEA Results	FOS	Acceptable?
5	σ_{xt}	85000	2585.50	32.88	32.88
5	σ_{xc}	65000	2561.50	25.38	25.38
5	σ_{yt}	83000	15689.00	5.29	5.29
5	σ_{yc}	55000	13542.00	4.06	4.06
5	σ_{zt}	13000	6779.70	1.92	1.92
5	σ_{zc}	17000	7192.10	2.36	2.36
5	τ_{xy}	19000	1341.10	14.17	14.17
5	τ_{yz}	19000	4078.70	4.66	4.66
5	τ_{xz}	19000	3127.50	6.08	6.08

Note: Material Property and FEA Result values are all given in pounds per square inch (psi).

The “Acceptable?” guideline indicates if a given factor of safety is above (green) or below (red)

the NAB Factor of Safety plus twenty percent.

Appendix D – YP Test Plan

06 October 2004

Yard Patrol Propeller Test Plan – Fall 2004/Spring 2005

Introduction:

Composite bladed propeller design could be the next logical step in the progression of propeller technology. The end result of the following tests is to determine how well a composite bladed propeller compares to a nickel aluminum bronze (NAB) model. To establish a baseline and minimize variables, the following procedure is proposed. Each phase is comprised of tests; each test is comprised of runs. Details of each are in the following pages.

For each of these tests, certain data is required:

- Speed will be read from the GPS display;
- Revolutions per minute will be indicated by an infrared pickup apparatus;
- Torque will be calculated using shaft-mounted strain gages;
- Cavitation induced vibration will be observed with a hull-mounted accelerometer;
- And, a load determining device will be used for the bollard test portion.

For the composite bladed phase, embedded strain gages will provide the strain readings. All of these tests are planned for YP 677 over the course of six months to allow for consistency in the engines, shaft gear, and resistance due to hull roughness and wetted surface area.

Phase Outlines:**Phase I:**

Baseline Data – Nickel Aluminum Bronze (NAB) Propellers

Timeline:

12-13 October 2004 – Instrumentation

15 October 2004 – Launch of YP 677

18-20 October 2004 – Baseline Trials

Objectives:

In order for subsequent tests to be of any value, a baseline must be established. Using two NAB propellers on YP 677, the entire test sequence will occur and corresponding observations and calculation will be made. As closely as possible following the end of this test, YP 677 will be removed from the water to replace the NAB propellers with the encapsulated propellers.

Phase II:

Encapsulated Propellers

Timeline:

21-22 October 2004 – Mount encapsulated propellers on YP

22-27 October 2004 – First set of trials

11-14 November 2004 – Second set of trials

11-14 December 2004 – Third set of trials (with induced damage)

Objectives:

The two primary objectives of these exercises are: 1) compare the encapsulated and NAB propellers in acceleration, strength, and fuel economy; and, 2) observe the durability of the encapsulated propellers' urethane coating. The first of the objectives serves as a template for the later composite bladed propeller tests. Results obtained from these – and the NAB – runs will serve as the baseline for the composite bladed tests and for age-dependent tests with the particular encapsulated propellers. Additionally, the comparison of these criteria indicates to what extent the urethane coating actually affects the propeller performance. Previous studies have shown that the coating may change the cavitation characteristics. Such properties might give the propeller increased speed at a given rate of rotation and better acceleration.

The second portion of the trial will indicate how well the urethane coating endures both the saltwater environment and the consistently harsh treatment by those who use the vessel on a daily basis. The Severn River tends to support relatively fast bio-fouling, making the three month timeframe sufficient to observe the effect on the propellers. An effort will be made to determine if there the specific advantages of both the stainless steel encapsulated propeller (SSENCAP) and the nickel-aluminum-bronze encapsulated propeller (NABENCAP). Finally, the bond between the urethane coating and metallic blade surface will be analyzed, especially if

impact occurs. If the propeller remains undamaged by the third test, damage will be induced by scraping or cutting the encapsulation to the metal core.

These propellers have no serial numbers, but they are a complimentary set. One is stainless steel, the other NAB, and both are coated with Versalink P1000 polyurethane.

Phase III:

Composite Bladed Propeller

Timeline:

February 2005 – Clean hull and mount composite bladed propeller on YP 677

February 2005 – Propeller Trials

Objectives:

The composite bladed tests will take place on a different Yard Patrol craft for two primary reasons. First of all, there will be only one composite bladed propeller, so there is an inherent baseline with the other propeller being NAB. The NAB propeller will be from the earlier YP 677 tests, creating further similarity among the phases. Two sets of tests will run: one on each propeller for the given hull. There is a large variation in hull roughness between YP hulls, so using the same hull is crucial. The purpose of this test is to compare the performance of the NAB model to the composite version, using the same standards established in the previous two phases. Upon completion of the test sequence, a diver will enter the water to inspect the composite propeller for signs of damage, due to the loading or impact. It is important to note in this case how well the composite material is withstanding the propulsive loads, especially

compared to the NAB model. On the same token, this is only a small snapshot in the service life of the propeller. The trials must push the composite bladed design to its limits, but further study will be necessary.

Procedure:

1. Mount the appropriate external sensors. **(DIVER)**
2. Mount the appropriate propeller to the designated YP.
3. Make initial observations, specifically on the used NAB propellers. Note any damage (ie. Pitted sections, deformed areas, gouges, etc.) **(DIVER)**
4. Proceed to designated testing area.
5. Commence Stage X. (See stage descriptions on following pages.)
6. Debrief stage, if necessary. Adjust location for following stage.
7. Repeat steps four and five until all stages are complete.
8. Secure from phase.
9. Complete post-phase observations. **(DIVER)**

Stage 1: Powering and Fuel Economy

1. At the OOD's discretion, commence the run in accordance with given instructions.
2. The run duration will be approximately five (5) minutes.
3. Collect data pertaining to torque, number of rotations per minute, speed of the vessel, heading, strain information (if applicable), and power supplied by the engines to their respective shafts.

4. Upon completion of the first leg, the vessel will return on a 180 degree (relative) track for five minutes.
5. Repeat until all runs are complete.
6. Secure from Stage 1.

Stage 2: Acceleration

1. At the OOD's discretion, commence the run in accordance with given instructions.
2. The run duration will be less than three (3) minutes.
3. From a stand-still, order All Ahead Flank.
4. Collect data pertaining to torque, number of rotations per minute, time until prescribed speed of the vessel, strain information (if applicable), and heading.
5. Repeat until all runs are complete.
6. Secure from Stage 2.

Stage 3: Emergency Stop

1. At the OOD's discretion, commence the run in accordance with given instructions.
2. The run duration will be approximately seven (7) minutes.
3. Accelerate the vessel to its maximum speed.
4. When approval is given by the test director, the OOD will order All Engines Back Full.

5. Collect data pertaining to torque, number of rotations per minute, time from stop order is given until vessel's velocity equals zero, strain information (if applicable), and heading.
6. Repeat until all runs are complete.
7. Secure from Stage 3.

Stage 4: Full Rudder Circles

1. At the OOD's discretion, commence the run in accordance with given instructions.
2. The run duration will be approximately seven (7) minutes.
3. When approval is given by the test director, the OOD will give the command for Full Rudder, direction depending on the test outline.
4. Collect data pertaining to torque, speed of the vessel, strain information (if applicable) and number of rotations per minute.
5. Once the vessel makes a full circle, the run is complete.
6. Repeat until all runs are complete.
7. Secure from Stage 4.

Stage 5: Bollard Test

1. At the OOD's discretion, commence the run in accordance with given instructions.
2. The run duration will be four (4) minutes.

3. Rig the fantail with TOWEX line and attach it to the designated bollard on the seawall.
4. When approval is given by the test director, the OOD will give the command for the prescribed engine bell.
5. Collect data pertaining to torque, revolutions per minute, strain information (if applicable), and the tension on the towing line.
6. Once the time period is over, the run is complete.
7. Repeat until all runs are complete.
8. Secure from Stage 5.

Stage 6: Cavitation Inception

1. At the OOD's discretion, commence the run in accordance with given instructions.
2. The run duration will be approximately five (5) minutes.
3. When approval is given by the test director, the OOD will give the command for the prescribed engine bell.
4. Collect data pertaining to torque, revolutions per minute, accelerometer readings, and strain information (if applicable).
5. At the discretion of the test director, the run is considered complete.
6. Repeat until all runs are complete.
7. Secure from Stage 6.

Stage 7: Operational Use

1. At the OOD's discretion, commence the run in accordance with given instructions.
2. The run duration will be fifteen (15) minutes.
3. When approval is given by the test director, the OOD will give commands, varying both rudder angle and speed.
4. Collect data pertaining to torque, revolutions per minute, strain information (if applicable), and speed of the vessel.
5. The run is considered complete when time expires.
6. Repeat until all runs are complete.
7. Secure from Stage 7.

Crew Requirements:

Support from NAVSTA Annapolis is an integral portion of this test. At least five (5) enlisted crew members are needed, including a senior enlisted leader. These individuals will be responsible for rigging and maneuvering the ship as required by the testing procedure.

Additionally, diver support is required, as indicated. The pilothouse will maintain a log of all course and speed changes, both during the test and during regular usage. Once the phase is complete, logging vessel activity is important for further damage analysis. The Officer of the Deck (OOD) and test director will be MIDN 1/c Michael Sammataro and MIDN 1/C Christopher Wozniak, respectively. Data collection will be overseen by MIDN Wozniak, as well, with guidance from personnel at NSWC Carderock Division. Upon the conclusion of the exercise, the

crew will be debriefed as to the success of the data collection and the possible need for future testing.

Administrative Notes:

Rudder and engine control directions will be outlined by the test director. The order of these tests is unimportant; depending on sea traffic and weather, each stage can take place at different times. The detailed agenda is forthcoming. Strain information will only be collected from the composite bladed propeller. Additional runs may be necessary for certain stages. The testing area will be determined and outlined by the test director.

Appendix E – Data Analysis Code

```

Sub Data_Processor_YP677()
Dim rowcounter1, samplecounter, counter As Integer
Dim sample As Range
Dim counter3, counter4, counter5, counter6, counter7, maxres, counter10, counter11, counter12
As Integer
Dim maxrow, maxtime, wksnum As Integer

*****
*****
'Control Module
If Worksheets("Control").Cells(2, 2) = 1 Then
    resfilename = "NAB I Results.xls"
    pfilename = "NAB Data Processing I.xls"
    fullresfn = "C:\Documents and Settings\Chris\Important Files\Trident Files\Excel Files\NAB I
Results.xls"
Else
    If Worksheets("Control").Cells(2, 2) = 2 Then
        resfilename = "ENCAP Results.xls"
        pfilename = "ENCAP Data Processing.xls"
        fullresfn = "C:\Documents and Settings\Chris\Important Files\Trident Files\Excel
Files\ENCAP Results.xls"
    End If
End If

maxwks = Worksheets("Control").Cells(2, 5) + 1
resmaxwks = Worksheets("Control").Cells(3, 5)
opuse = Worksheets("Control").Cells(4, 5)
desiredout = Worksheets("Control").Cells(5, 5)
rho = Worksheets("Control").Cells(7, 5)
d = Worksheets("Control").Cells(8, 5)
spikebuffer = Worksheets("Control").Cells(9, 5)

analysisopt = Worksheets("Control").Cells(3, 2)
compileopt = Worksheets("Control").Cells(4, 2)
chartopt = Worksheets("Control").Cells(5, 2)
buildarr = Worksheets("Control").Cells(6, 2)
spikecont = Worksheets("Control").Cells(7, 2)
*****
*****

```

```
*****
```

```
*****
```

```
***Repeats process for all worksheets
```

```
If analysisopt = 1 Then
```

```
For wksnum = 2 To maxwks
```

```
    maxrow = 2
```

```
    maxtime = 2
```

```
    Workbooks(pfilename).Worksheets(wksnum).Activate
```

```
*****
```

```
***
```

```
***Format Module
```

```
Worksheets(2).Select
```

```
Rows("1:1").Select
```

```
Range("F1").Activate
```

```
Selection.Copy
```

```
Worksheets(wksnum).Select
```

```
Cells(1, 1).Select
```

```
ActiveSheet.Paste
```

```
Selection.PasteSpecial Paste:=xlPasteColumnWidths, Operation:=xlNone, _  
    SkipBlanks:=False, Transpose:=False
```

```
***Center justifies data
```

```
Cells.Select
```

```
With Selection
```

```
    .HorizontalAlignment = xlGeneral
```

```
    .VerticalAlignment = xlBottom
```

```
    .WrapText = False
```

```
    .Orientation = 0
```

```
    .AddIndent = False
```

```
    .IndentLevel = 0
```

```
    .ShrinkToFit = False
```

```
    .ReadingOrder = xlContext
```

```
    .MergeCells = False
```

```
End With
```

```
With Selection
```

```
    .HorizontalAlignment = xlCenter
```

```
    .VerticalAlignment = xlBottom
```

```
    .WrapText = False
```

```
    .Orientation = 0
```

```
    .AddIndent = False
```

```

.IndentLevel = 0
.ShrinkToFit = False
.ReadingOrder = xlContext
.MergeCells = False
End With

```

```

*****
***

```

```

***Find Boundary Module

```

```

***Voltage Data

```

```

If wksnum = opuse Then
  Do
    maxrow = maxrow + 1
    Loop Until Cells(maxrow, 4) = 0 And Cells(maxrow + 1, 4) = 0 And Cells(maxrow + 2,
4) = 0 And Cells(maxrow + 3, 4) = 0 And maxrow > 20000
  Else
    Do
      maxrow = maxrow + 1
      Loop Until Cells(maxrow, 4) = 0 And Cells(maxrow + 1, 4) = 0 And Cells(maxrow + 2,
4) = 0 And maxrow > 1500
    End If
  End If

```

```

***Time Data

```

```

Do
  maxtime = maxtime + 1
  Loop Until Cells(maxtime, 3) = 0 And maxtime > 100

```

```

maxtime = maxtime - 1
maxrow = maxrow - 10
Cells(22, 22) = maxtime

```

```

*****
***

```

```

*****
***

```

```

***Spike Control Module

```

```

If spikecont = 1 Then
  counter20 = 0
  Do
    counter20 = counter20 + 1
    Loop Until Cells(counter20 + 1, 4) = 0 And Cells(counter20 + 2, 4) = 0

```

```

For rcounter = 2 To counter20
  If Cells(rcounter, 4) <= spikebuffer Then
    Cells(rcounter, 4) = Application.WorksheetFunction.Average(Range(Cells(rcounter -
3, 4), Cells(rcounter - 1, 4)))
  End If
  If Cells(rcounter, 5) <= spikebuffer Then
    Cells(rcounter, 5) = Application.WorksheetFunction.Average(Range(Cells(rcounter -
3, 5), Cells(rcounter - 1, 5)))
  End If
Next rcounter
End If

```

```

'*****
***

```

```

'*****
***

```

```

'***Averaging Module
samplecounter = 2
counter = 2
For counter3 = 2 To maxtime
  For rowcounter = 2 To maxrow
    If rowcounter = samplecounter Then
      Cells(counter, 8) = Application.WorksheetFunction.Average(Range(Cells(rowcounter,
4), Cells(rowcounter + 9, 4)))
      Cells(counter, 9) = Application.WorksheetFunction.Average(Range(Cells(rowcounter,
5), Cells(rowcounter + 9, 5)))
      Cells(counter, 10) = 1180.19 * Cells(counter, 8)
      Cells(counter, 11) = 1180.19 * Cells(counter, 9)
      counter = counter + 1
    End If
  Next rowcounter
  samplecounter = samplecounter + 10
Next counter3

```

```

'*****
***

```

```

'*****
***

```

```

'***RPM Procedure

```

```

counter5 = 2
For counter4 = 3 To maxtime
  time1 = Cells(counter5, 3)
  time2 = Cells(counter4, 3)
  cell1 = Cells(counter4 - 1, 6)
  cell2 = Cells(counter4, 6)
  cell3 = Cells(counter4 - 1, 7)
  cell4 = Cells(counter4, 7)
  If cell2 > cell1 Or cell4 > cell3 Then
    Cells(counter4, 14) = (cell2 - cell1) / (time2 - time1)
    Cells(counter4, 15) = (cell4 - cell3) / (time2 - time1)
    counter5 = counter4
  End If
Next counter4

```

```

*****
***

```

```

*****
***

```

```

*** KQ Procedure

```

```

counter7 = 2
For counter6 = 2 To maxtime
  If Cells(counter6, 14) > 0 Then
    sqavg = Application.WorksheetFunction.Average(Range(Cells(counter7, 10),
Cells(counter6, 10)))
    pqavg = Application.WorksheetFunction.Average(Range(Cells(counter7, 11),
Cells(counter6, 11)))
    Cells(counter6, 12) = sqavg
    Cells(counter6, 13) = pqavg
    srpm = Cells(counter6, 14)
    prpm = Cells(counter6, 15)

    If srpm > 0 Then
      Cells(counter6, 16) = Abs(sqavg / (rho * ((srpm / 60) ^ 2) * (d ^ 5)))
    Else
      If srpm = 0 Or srpm < 0 Then Cells(counter6, 16) = 0
    End If

    If prpm > 0 Then
      Cells(counter6, 17) = Abs(pqavg / (rho * ((prpm / 60) ^ 2) * (d ^ 5)))
    Else

```

```

    If prpm = 0 Or srpm < 0 Then Cells(counter6, 17) = 0
  End If

```

```

    counter7 = counter6 + 1
  End If
Next counter6

```

```

'*****
***

```

```

'*****
***

```

```

'***J Procedure

```

```

counter9 = 2
For counter8 = 2 To maxtime
  If Cells(counter8, 14) > 0 Then
    va = Cells(counter9, 2) * 1.689
    sn = Cells(counter8, 14) / 60
    pn = Cells(counter8, 15) / 60

    If sn > 0 Then
      Cells(counter8, 18) = Abs(va / (sn * d))
    Else
      If sn = 0 Or sn < 0 Then Cells(counter8, 18) = 0
    End If

    If pn > 0 Then
      Cells(counter8, 19) = Abs(va / (pn * d))
    Else
      If pn = 0 Or pn < 0 Then Cells(counter8, 19) = 0
    End If
    counter9 = counter9 + 1
  End If
Next counter8

```

```

'*****
***

```

```

'***Power Procedure

```

```

For counter8 = 2 To maxtime
  If Cells(counter8, 14) > 0 Then
    sq = Cells(counter8, 12)
    pq = Cells(counter8, 13)

```

```

    sn = Cells(counter8, 14) / 60
    pn = Cells(counter8, 15) / 60

    Cells(counter8, 20) = Abs(sq * sn * 2 * 3.14159265358979 / 550)
    Cells(counter8, 21) = Abs(pq * pn * 2 * 3.14159265358979 / 550)
  End If
Next counter8
Next wksnum

End If
'*****
*****

'*****
*****

'***Create Results Workbook
If compileopt = 1 Then

Workbooks.Open Filename:= _
    fullresfn

For wksnum = 2 To resmaxwks + 1

'*****
***

'***Format Module

'***Sets header
For wksnum1 = 2 To resmaxwks + 1
  Workbooks(resfilename).Activate
  Worksheets(1).Select
  Rows("1:1").Select
  Range("F1").Activate
  Selection.Copy
  Worksheets(wksnum1).Select
  Cells(1, 1).Select
  ActiveSheet.Paste
  Selection.PasteSpecial Paste:=xlPasteColumnWidths, Operation:=xlNone, _
    SkipBlanks:=False, Transpose:=False
Next wksnum1

'***Center justifies data
Cells.Select
With Selection
  .HorizontalAlignment = xlGeneral

```

```

.VerticalAlignment = xlBottom
.WrapText = False
.Orientation = 0
.AddIndent = False
.IndentLevel = 0
.ShrinkToFit = False
.ReadingOrder = xlContext
.MergeCells = False
End With
With Selection
.HorizontalAlignment = xlCenter
.VerticalAlignment = xlBottom
.WrapText = False
.Orientation = 0
.AddIndent = False
.IndentLevel = 0
.ShrinkToFit = False
.ReadingOrder = xlContext
.MergeCells = False
End With

*****
***Data Compiler

counter11 = 2
'wksnum = reswksnum + 1
maxtime = Workbooks(pfilename).Worksheets(wksnum).Cells(22, 22)
Workbooks(pfilename).Worksheets(wksnum).Activate
Columns(2).Select
Selection.Copy
Workbooks(resfilename).Worksheets(wksnum - 1).Activate
Cells(1, 1).Select
ActiveSheet.Paste
  For counter10 = 2 To maxtime
    If Workbooks(pfilename).Sheets(wksnum).Cells(counter10, 14) > 0 Then
      Workbooks(resfilename).Worksheets(wksnum - 1).Cells(counter11, 2) =
Workbooks(pfilename).Sheets(wksnum).Cells(counter10, 14)
      Workbooks(resfilename).Worksheets(wksnum - 1).Cells(counter11, 3) =
Workbooks(pfilename).Sheets(wksnum).Cells(counter10, 15)
      Workbooks(resfilename).Worksheets(wksnum - 1).Cells(counter11, 4) =
Workbooks(pfilename).Sheets(wksnum).Cells(counter10, 18)
      Workbooks(resfilename).Worksheets(wksnum - 1).Cells(counter11, 5) =
Workbooks(pfilename).Sheets(wksnum).Cells(counter10, 19)
      Workbooks(resfilename).Worksheets(wksnum - 1).Cells(counter11, 6) =
Workbooks(pfilename).Sheets(wksnum).Cells(counter10, 16)
    End If
  Next counter10
End Sub

```

```

        Workbooks(resfilename).Worksheets(wksnum - 1).Cells(counter11, 7) =
Workbooks(pfilename).Sheets(wksnum).Cells(counter10, 17)
        Workbooks(resfilename).Worksheets(wksnum - 1).Cells(counter11, 10) =
Workbooks(pfilename).Sheets(wksnum).Cells(counter10, 20)
        Workbooks(resfilename).Worksheets(wksnum - 1).Cells(counter11, 11) =
Workbooks(pfilename).Sheets(wksnum).Cells(counter10, 21)
        counter11 = counter11 + 1
    End If
Next counter10
Next wksnum

```

```

*****
*** RPM Deviation Calculator

```

```

Workbooks(resfilename).Activate

```

```

wksnum = 1

```

```

Do

```

```

    rescounter = 0

```

```

    Do

```

```

        rescounter = rescounter + 1

```

```

    Loop Until Worksheets(wksnum).Cells(rescounter, 2) = 0

```

```

    Worksheets(wksnum).Cells(100, 1) = rescounter

```

```

For counter12 = 2 To Worksheets(wksnum).Cells(100, 1) - 1

```

```

    Worksheets(wksnum).Activate

```

```

    spd1 = Cells(counter12, 1)

```

```

    srpm1 = Cells(counter12, 2)

```

```

    prpm1 = Cells(counter12, 3)

```

```

    sbhp1 = Cells(counter12, 10)

```

```

    pbhp1 = Cells(counter12, 11)

```

```

    Worksheets(wksnum + 1).Activate

```

```

    spd2 = Cells(counter12, 1)

```

```

    srpm2 = Cells(counter12, 2)

```

```

    prpm2 = Cells(counter12, 3)

```

```

    sbhp2 = Cells(counter12, 10)

```

```

    pbhp2 = Cells(counter12, 11)

```

```

    spdavg = Application.WorksheetFunction.Average(spd1, spd2)

```

```

    srpmavg = Application.WorksheetFunction.Average(srpm1, srpm2)

```

```

    prpmavg = Application.WorksheetFunction.Average(prpm1, prpm2)

```

```

    sbhpavg = Application.WorksheetFunction.Average(sbhp1, sbhp2)

```

```

    pbhpavg = Application.WorksheetFunction.Average(pbhp1, pbhp2)

```

```

    oprpm = (0.0341 * spdavg ^ 3) - (0.0421 * spdavg ^ 2) + (25.333 * spdavg)

```

```

    If oprpm > 0 Then

```

```

        Cells(counter12, 8) = 100 * (oprpm - srpmavg) / oprpm
    End If

```

```

Cells(counter12, 9) = 100 * (oprpm - prpmavg) / oprpm
Else
    Cells(counter12, 8) = 0
    Cells(counter12, 9) = 0
End If
Cells(counter12, 12) = spdavg * 1.689 / (sqrt(32.2 * 101.2))
Cells(counter12, 13) = sbhpavg
Cells(counter12, 14) = pbhpavg
Cells(counter12, 15) = srpmavg
Cells(counter12, 16) = prpmavg
Next counter12
wksnum = wksnum + 2
Loop While wksnum < resmaxwks

End If
*****

*****

***Combined Data Sheet Builder

If buildarr = 1 Then

    If compileopt < 1 Then Workbooks.Open Filename:= _
        fullresfn

rowcounter = 2
Workbooks(resfilename).Activate

wksnum1 = 1
For wksnum = 1 To resmaxwks
    counter = 0
    Do
        counter = counter + 1
    Loop Until Worksheets(wksnum).Cells(counter + 1, 3) = 0

    For counter1 = 2 To counter
        colcounter = 1
        For counter2 = 1 To desiredout + 1
            Worksheets("Combined Data").Cells(rowcounter, colcounter) =
Workbooks(wksnum).Cells(counter1, counter2)
            colcounter = colcounter + 1
        Next counter2
        rowcounter = rowcounter + 1
    Next counter1
    wksnum1 = wksnum + 2

```

Next wksnum

End If

End Sub